

NATIONAL TRANSPORTATION SAFETY BOARD

Office of Research and Engineering
Materials Laboratory Division
Washington, D.C. 20594



October 24, 2018

MATERIALS LABORATORY FACTUAL REPORT

Report No. 18-082

A. ACCIDENT INFORMATION

Place : Miami, Florida
Date : March 15, 2018
Vehicle : Florida International University UniversityCity Pedestrian Bridge
NTSB No. : HWY18MH009
Investigator : Robert Accetta (HS-20)

B. COMPONENTS EXAMINED

1. Documentation of the locations and extraction of samples for materials testing from the bridge.
2. Summary of 'Turner-Fairbank Highway Research Center Factual Report: Steel and Concrete Materials Testing'.

C. DETAILS OF THE EXAMINATION

SAMPLE LOCATION AND EXTRACTION

Span 1 of the Florida International University (FIU) UniversityCity Pedestrian Bridge linking the city of Sweetwater, Florida to the campus of FIU collapsed several days after placement onto elevated piers. The bridge was a post-tensioned concrete structure that included steel post-tensioning (PT) rods and tendons embedded in high-strength concrete. The bridge was built adjacent to the site and then moved into place using accelerated bridge construction (ABC) methods.

After the collapse, numerous samples of concrete and steel from the bridge were collected on-site for future materials testing. As shown in Figure 1, the north end of the bridge had sizeable portions of structure largely intact, and the majority of samples came from this area. In this area, the northmost portion of the bridge containing Diagonal 11, Vertical 12, and the canopy between those two members had rotated 90 degrees counterclockwise, as viewed looking west, from the original intact bridge position.

Four large-scale pieces were collected from the bridge on-scene as intact as possible. The four large scale pieces were the following:

- Diagonal 11 (top image, Figure 2)
- Blister 10/11 (bottom image, Figure 2)
- Vertical 12 (Figure 3)
- The northmost portion of the deck that included the nodal region where Diagonal 11 and Vertical 12 met the deck (Figures 4-7)

Diagonal 11 was obtained by torch cutting the PT rods at the top end of the member, then lifting it via crane. Blister 10/11 was obtained by jackhammering the concrete along the bottom edge to separate it from the top of the mating canopy, torch cutting the PT rods and reinforcing bars along the bottom of the blister, then lifting it via crane.

Before obtaining the additional large-scale pieces, the northmost portion of the bridge that still had Vertical 12 connected to the mating canopy had to be repositioned. This portion of the bridge was flipped so it was resting on the top of the canopy, with Vertical 12 sticking up, which is 180 degrees from the original intact bridge position. A brief sequence of this operation is shown in the top of Figure 3. The top surface of Vertical 12 was then sectioned from the mating canopy using a diamond rope saw, the PT rods were torch cut, and Vertical 12 was then lifted via crane.

The center two-thirds of the northmost portion of the deck was wet saw cut from the remainder of the structure, as shown in Figure 4. This area was where Diagonal 11 and Vertical 12 met the deck. Two large-diameter cores were sectioned from the concrete (bottom image of Figure 4) to provide “pick points” for lifting the piece, and to allow a crane to act as a stabilizing force during final cutting (Figure 5). Once the cuts were complete, the concrete of the deck surrounding the cuts was removed via jackhammer to facilitate removal of the piece. When clearance was obtained, the deck piece was removed via crane using the pick points (Figures 6-7).

All of the large-scale specimens were transported via flatbed trucks to a Florida Department of Transportation (FDOT) yard for future work and long-term storage.

Concrete core samples for materials testing were taken from the east and west side of the bridge deck in the areas shown in Figures 8 and 9. A mix of eight partial and full samples were obtained. Four partial and full concrete core samples for materials testing were taken from the canopy in the areas shown in Figure 10.

The large-diameter concrete cores taken from the pick points of the deck are shown in Figures 11 and 12. These samples were retained in case further analysis was warranted.

Two pieces of concrete with smooth geometrical features were found on the north side of the collapse site, between the north pier and the canal bulkhead containment wall. Figure 13 shows the general vicinity on-scene where the pieces were found. The smooth features were consistent with concrete that had formed against a rounded internal component such as a drain pipe. The pieces were thus labeled Drain Pipe #1 and Drain Pipe #2 and were retained as evidence.

In addition to the concrete samples, numerous steel samples were also collected for materials testing. While on-scene, the top portion of the bottom PT rod from Diagonal 11 was saw cut and retained. This length of PT rod had the hydraulic jack from the post-

tensioning operation still assembled to it after the collapse¹. A length of virgin PT rod was collected from a stockpile of unused building materials being stored on the build site near the south end of the bridge. The stockpile was undisturbed by the collapse of the bridge. Both PT rods collected are shown in Figure 14.

After moving the large-scale specimens to the FDOT yard, steel reinforcing bars of various sizes were collected. Reinforcing bars of sizes #5, #7, and #8 were collected via torch cutting from either the deck piece or the bottom end of Diagonal 11. Reinforcing bars of size #11 were extracted from Vertical 12 by removing the concrete surrounding the bars via jackhammer, then saw cutting them. The bars collected from Diagonal 11 and Vertical 12 are marked with blue painter's tape and beige masking tape in Figures 15 and 16, respectively.

MATERIALS TESTING

The concrete cores and steel rods and bars were shipped to the Federal Highway Administration (FHWA) Turner-Fairbank Highway Research Center (TFHRC) in McLean, Virginia for materials testing. The TFHRC report that documents the materials testing is attached in Appendix A.

The materials testing was performed on two separate dates. Parties to the NTSB investigation were invited to observe the materials testing at the TFHRC facility on both occasions.

Per the UniversityCity Prosperity Project plans, the concrete for the canopy, members, and the deck was specified to be Class VI with a minimum 28-day compressive strength of 8,500 psi. All the concrete core specimens from both the deck and the canopy had compression test results that met this requirement.

There were no specifications for tensile strength of the concrete. However, the post-failure fracture surfaces of the tension specimens were all perpendicular to the direction of loading, which is typical of brittle materials like concrete that fail in tension.

The bridge design plans specified the concrete used had to be in accordance with Section 346 of the standard FDOT specifications². Per this specification, the air content of Class VI concrete is to be within the range of 1.0% to 6.0%. All specimens from both the deck and the canopy were within this range for total air content.

The post-tensioning rods were specified to be steel per ASTM A722³, Grade 150. Two types of specimens were tested: machined round bar specimens and full-size bar specimens. The two specimen types were prepared from both the virgin and Diagonal 11

¹ See NTSB Materials Laboratory Factual Report No. 18-081

² FDOT Standard Specifications for Road and Bridge Construction (July 2015). "Standard 346 – Portland Cement Concrete."

³ ASTM A722. (2014). "Standard Specification for Uncoated High-Strength Steel Bars for Prestressing Concrete." ASTM Annual Book of Standards 01.04. ASTM International. West Conshohocken, PA.

PT rods. For all the tension tests the specimens met the specified minimum yield strength, tensile strength, and percent elongation at fracture.

The chemical composition of the virgin and Diagonal 11 PT rods had levels of phosphorus and sulfur below the specified maximums for ASTM A722.

The reinforcing bars were specified to be steel per ASTM A615⁴, Grade 60. Collapse-induced deformation of the size #7 bars collected precluded testing of them. Tension test results of the remaining size #5, #8, and #11 bars all met the minimum yield strength, tensile strength, and percent elongation at fracture for their respective sizes.

In summary, the concrete and steel specimens tested by TFHRC researchers met the minimum requirements specified in the UniversityCity Prosperity Project build plans.

Adrienne V. Lamm
Materials Engineer

⁴ ASTM A615. (2014). "Standard Specification for Deformed and Plain Carbon-Steel Bars for Concrete Reinforcement." ASTM Annual Book of Standards 01.04. ASTM International. West Conshohocken, PA.



Figure 1: Photo looking west showing the north end of the bridge after collapse.

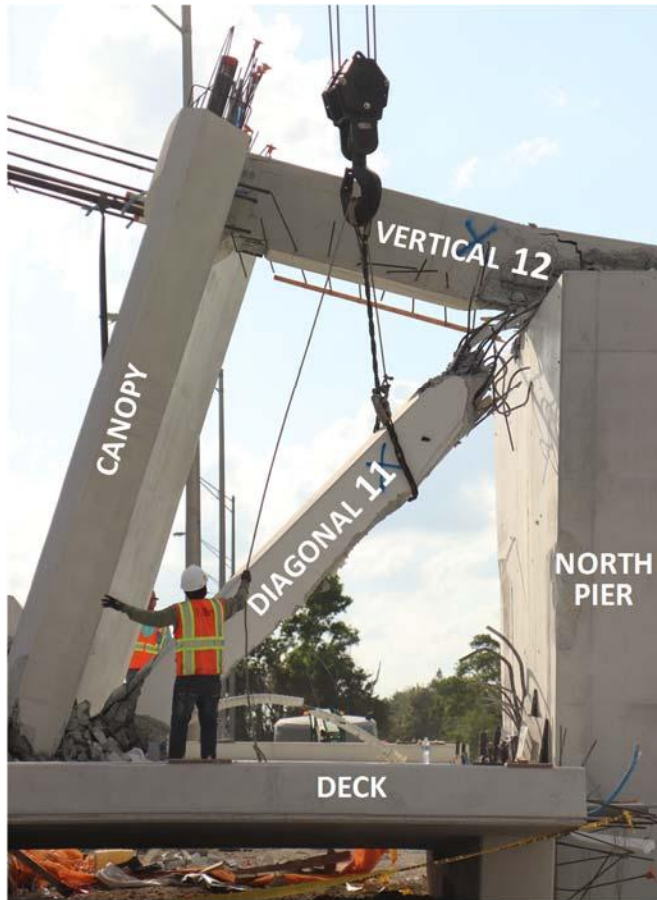


Figure 2: Photos looking west showing the removal via crane of Diagonal 11 (top) and Blister 10/11 (bottom).

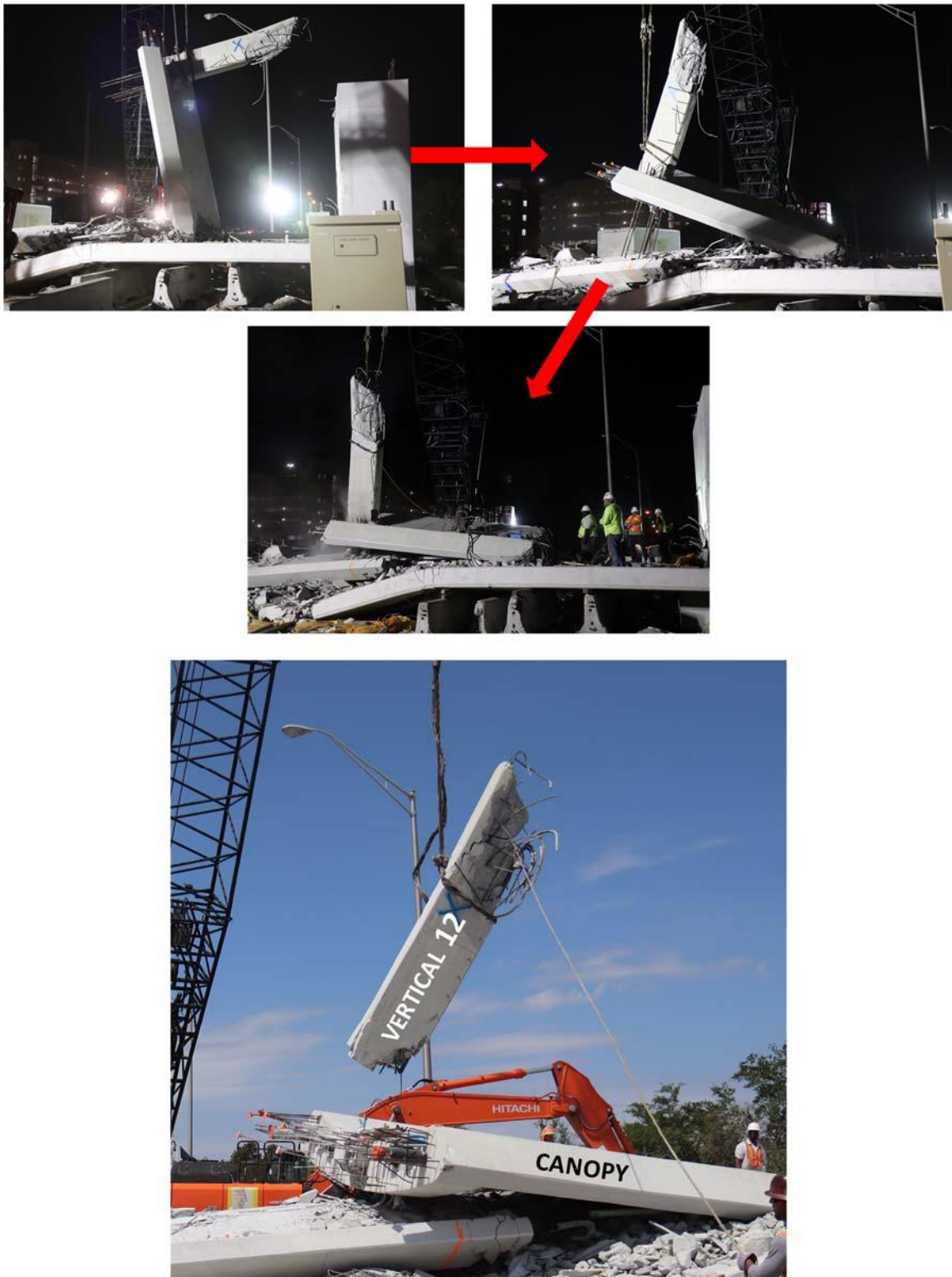


Figure 3: Photos looking west showing the operation to move the remaining north end of the bridge so it rests on top of the canopy (top three images) and the removal via crane of Vertical 12 (bottom image).



Figure 4: Photos showing the saw cut of the center two-thirds of the northmost portion of the deck. The two large-diameter cores taken to provide pick points for lifting the piece are indicated.



Figure 5: Photos looking west showing positioning of the crane for support and eventual removal of the large deck piece.

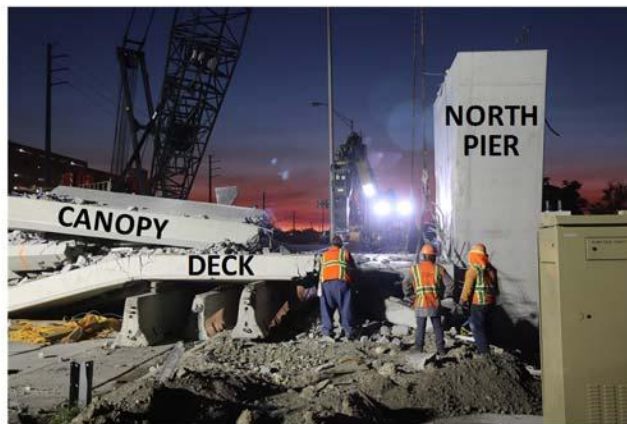


Figure 6: Photos looking west showing jackhammering and removal via crane of the large deck piece.

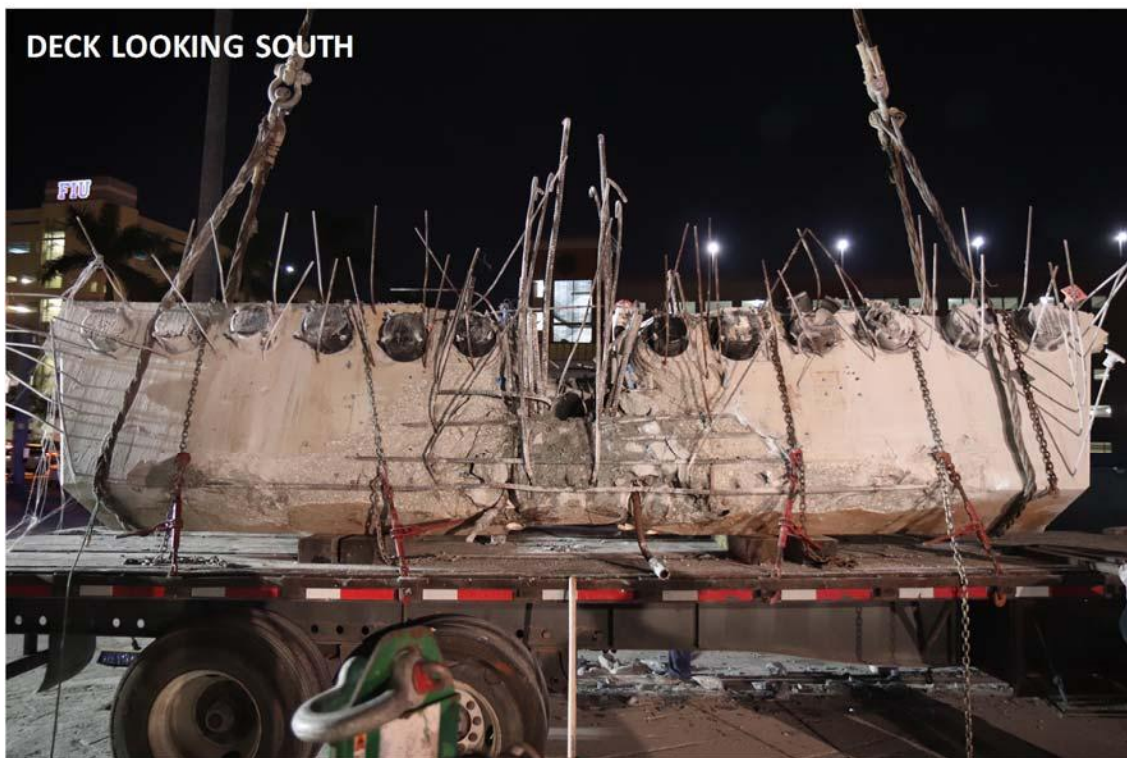
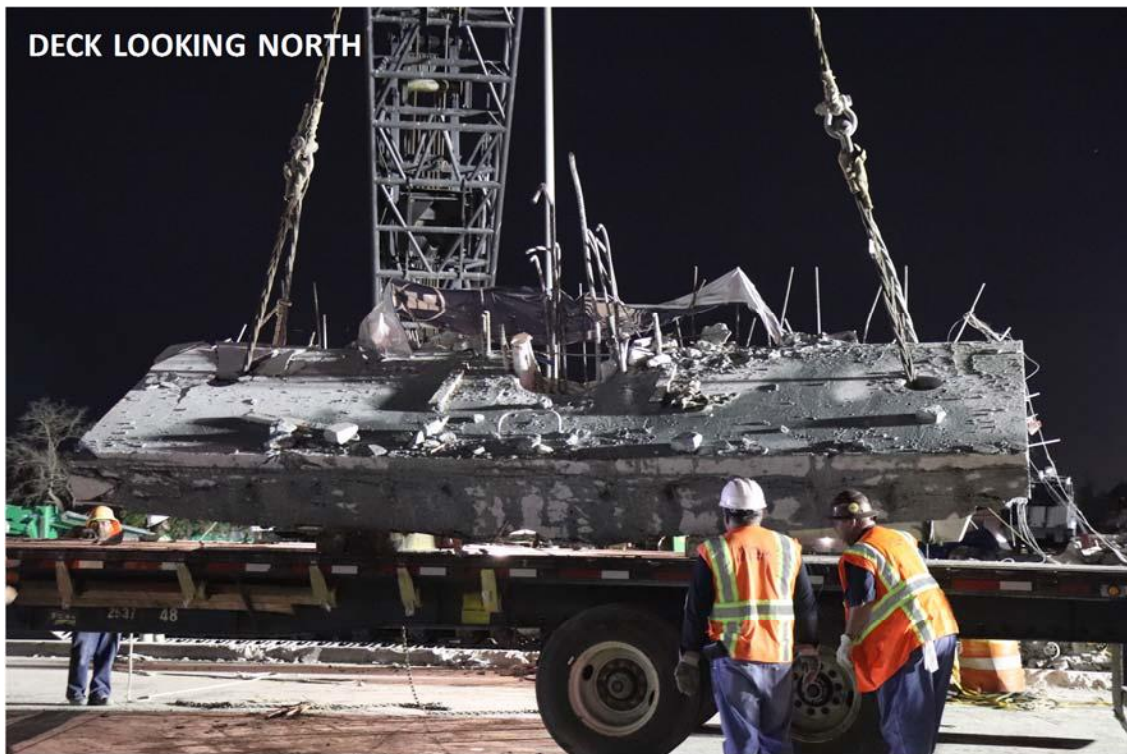


Figure 7: Photos showing the large deck piece after removal from the remaining bridge structure. Damage is visible on the north face of the deck.



Figure 8: Photos showing the marked locations where concrete core samples for materials testing were taken from the east and west side of the deck. Per the design plans and ultrasonic inspection, the indicated areas were clear of underlying steel and plastic conduit internal to the deck.

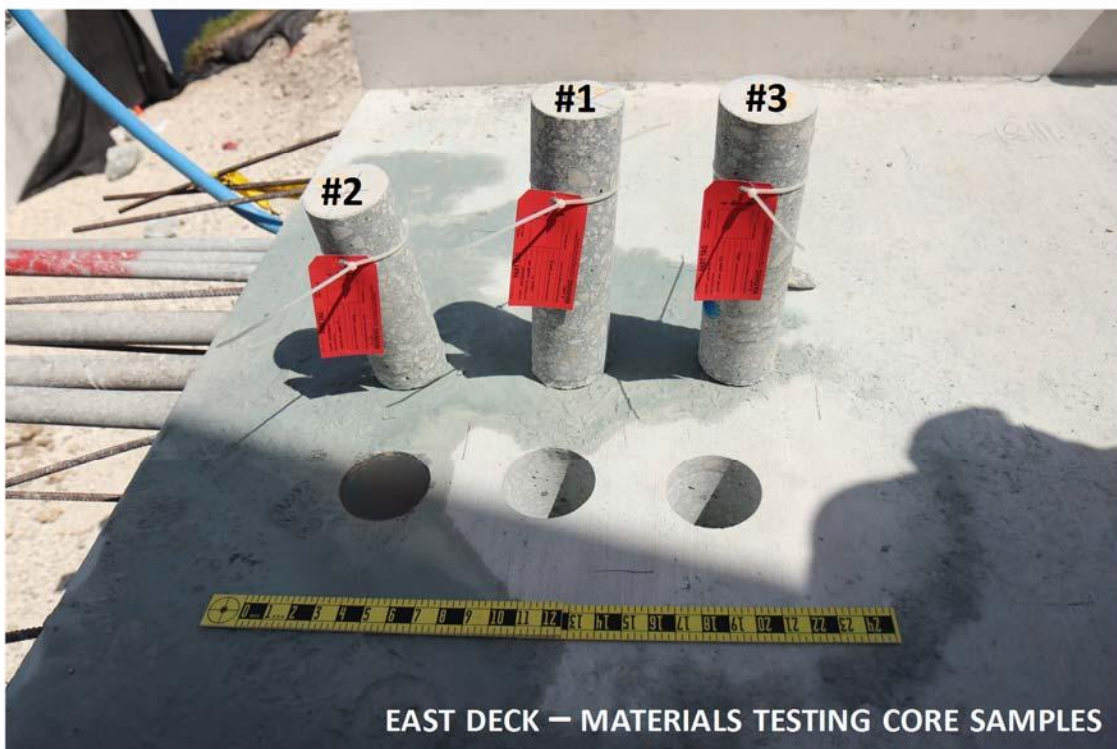
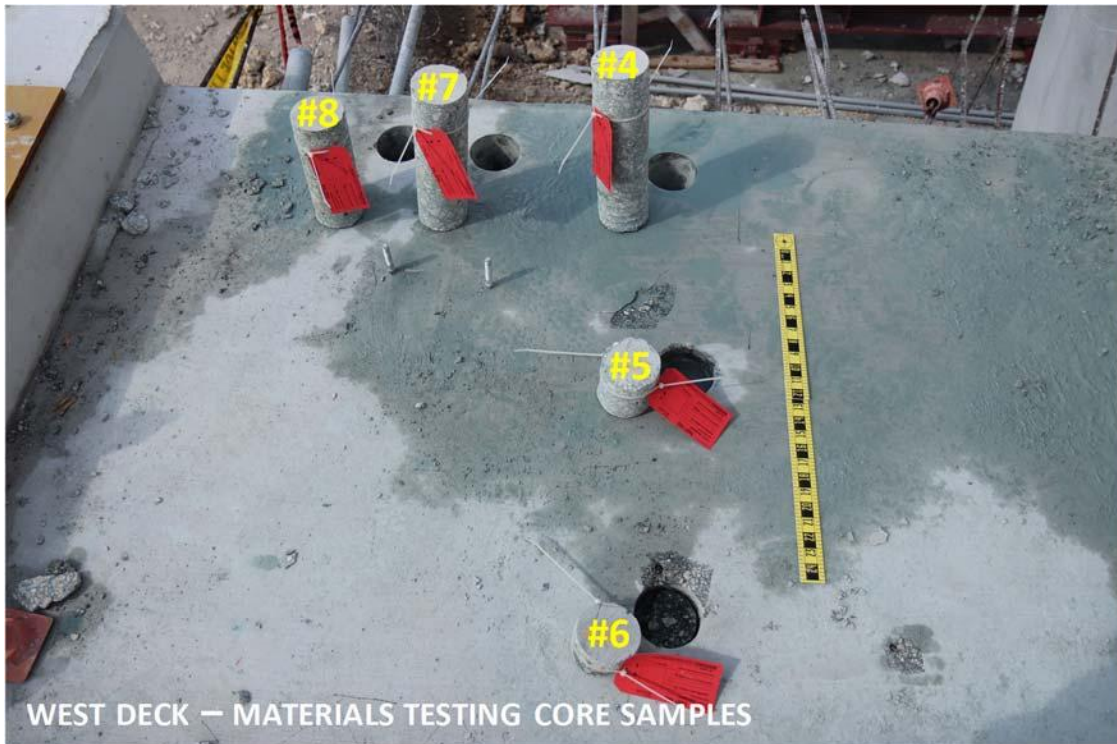


Figure 9: Photos showing the actual locations where concrete core samples for materials testing were taken from the east and west side of the deck on-scene.

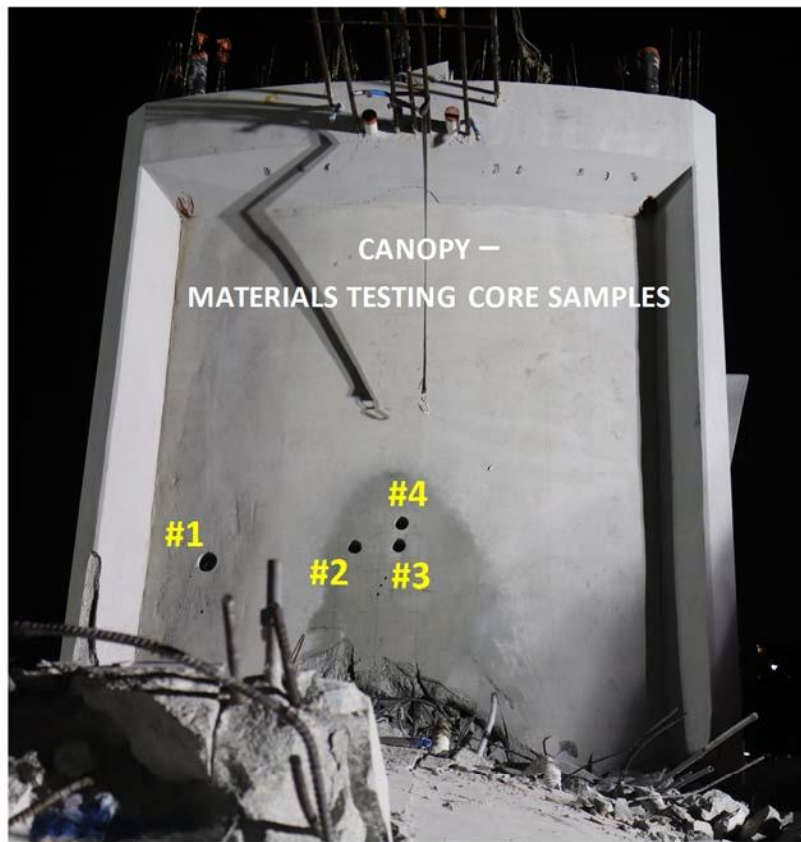


Figure 10: Photos showing the actual locations where concrete core samples for materials testing were taken from the canopy on-scene.



Figure 11: Photos showing the large deck piece after placement in the FDOT yard. Damage is visible on the north face of the deck. The locations of the large-diameter concrete cores that served as pick points for moving the piece are indicated.

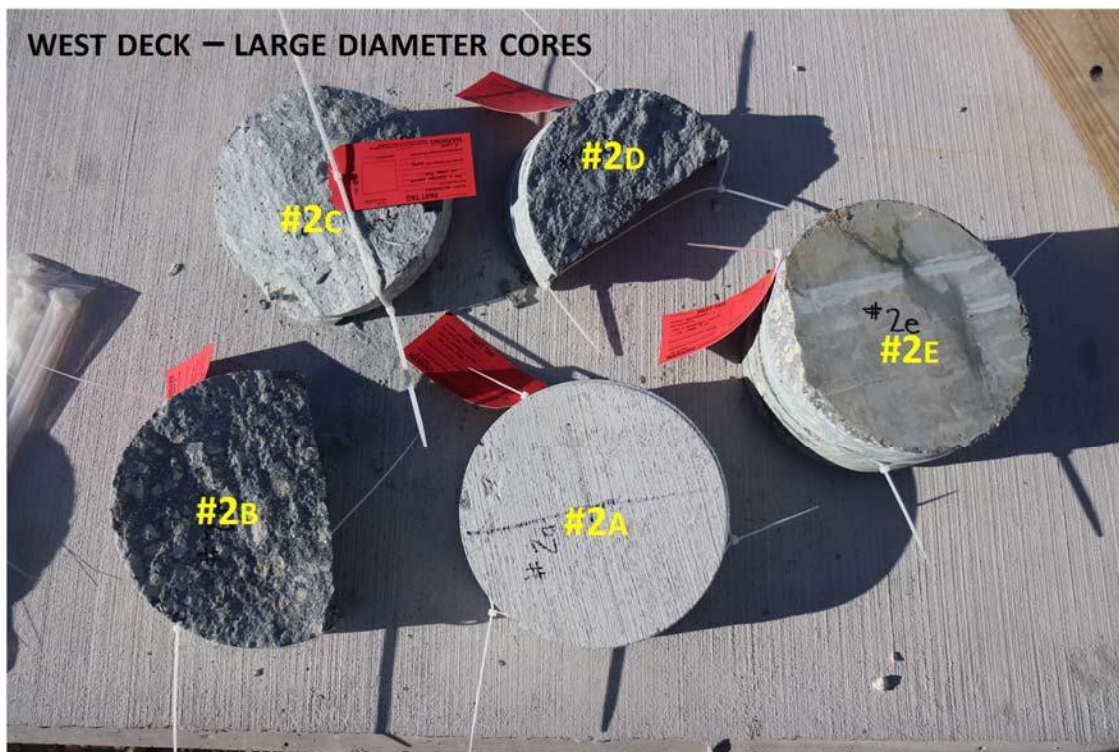
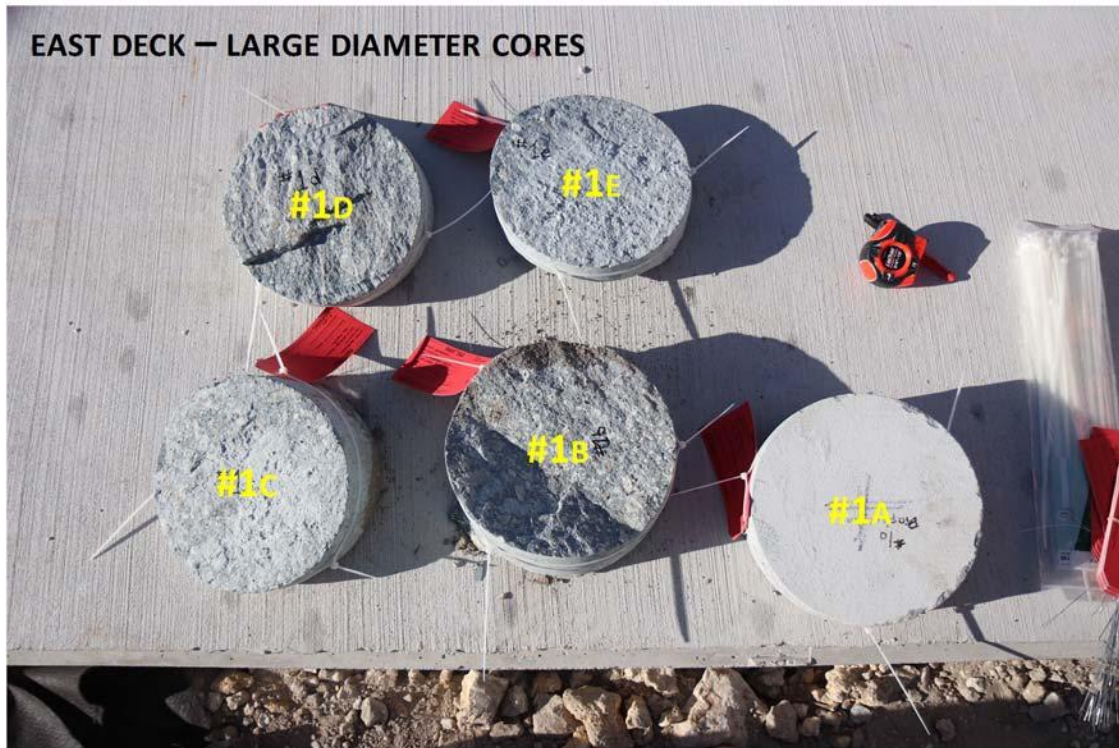


Figure 12: Photos showing the large-diameter concrete cores taken from the deck on-scene.



Figure 13: (Top) Photo showing the general location where two pieces of concrete with smooth geometrical features were found on the north side of the collapse site, between the north pier and the canal bulkhead containment wall. (Bottom) Photo showing the two pieces of concrete after handling and visual inspection.



Figure 14: Photos showing the on-scene removal of the bottom PT rod from Diagonal 11 (top) and the two PT rods shipped to TFHRC for testing (bottom).



Figure 15: (Top) Photo showing some of the reinforcing bars collected from Diagonal 11 while at the FDOT yard prior to sectioning. (Bottom) Photo showing some of the reinforcing bars collected from the pieces stored at the FDOT yard and sent to TFHRC for testing.



Figure 16: The top photo shows the location in Vertical 12 where the bars shown in the bottom photo were removed at the FDOT yard. The bars were sent to TFHRC for testing.

Appendix A:
Turner-Fairbank Highway Research Center Factual Report:
Steel and Concrete Materials Testing

TURNER-FAIRBANK HIGHWAY RESEARCH CENTER
FACTUAL REPORT
Steel and Concrete Materials Testing

Prepared For:

National Transportation Safety Board
NTSB Accident ID: HWY18MH009

Prepared by:

Justin Ocel, Ph.D., P.E.
Benjamin Graybeal, Ph.D., P.E.
Zachary Haber, Ph.D.

Federal Highway Administration
Turner-Fairbank Highway Research Center
6300 Georgetown Pike, McLean, VA 22101

October 14, 2018

TABLE OF CONTENTS

INTRODUCTION..... 1

SCOPE 2

CONCRETE CORES AND CYLINDERS 3

 Documentation 3

 Testing Plan 7

 Results 13

POST-TENSIONING RODS 24

 Documentation 24

 Test Plan..... 25

 Tension Test Method Description 28

 Tension Testing Results 30

 Hardness Results 34

 Chemical Analysis Results 37

REINFORCING BARS 38

 Documentation 38

 Tension Test Method Description 40

 Tension Test Results 40

INTRODUCTION

On March 15th 2018, Span 1 of a pedestrian bridge being constructed on the main Maimi campus of Florida International University (FIU) collapsed. The prefabricated bridge was to connect the FIU campus with the neighboring town of Sweetwater. The span that collapsed crossed over SW 8th Street and had been moved into place using self-propelled modular transports (SPMT) days before the collapse; shown in Figure 1. The span in its collapsed state is shown in Figure 2.

Investigators from the National Transportation Safety Board (NTSB) were dispatched to the scene. Engineers from the Federal Highway Administration (FHWA) were also dispatched to the scene to assist NTSB with the investigation. During the on-site investigation, evidence was collected which was to be later used to assist in determining the cause of the bridge failure. Some of that evidence included construction materials such as steel and concrete used to construct the structure.

Portions from the north end of the failed structure were retained and housed at a local Florida Department of Transportation (FDOT) maintenance yard for further investigation. NTSB investigators and FHWA engineers made multiple trips to this FDOT maintenance yard to further inspect the bridge segments and extract additional evidence, which included construction materials such as steel and concrete used to construct the structure.

The extracted construction materials were transported to the FHWA's Turner-Fairbank Highway Research Center (TFHRC) in McLean, Virginia for testing and assessment.



Figure 1. Span 1 of the FIU pedestrian bridge being moved into place

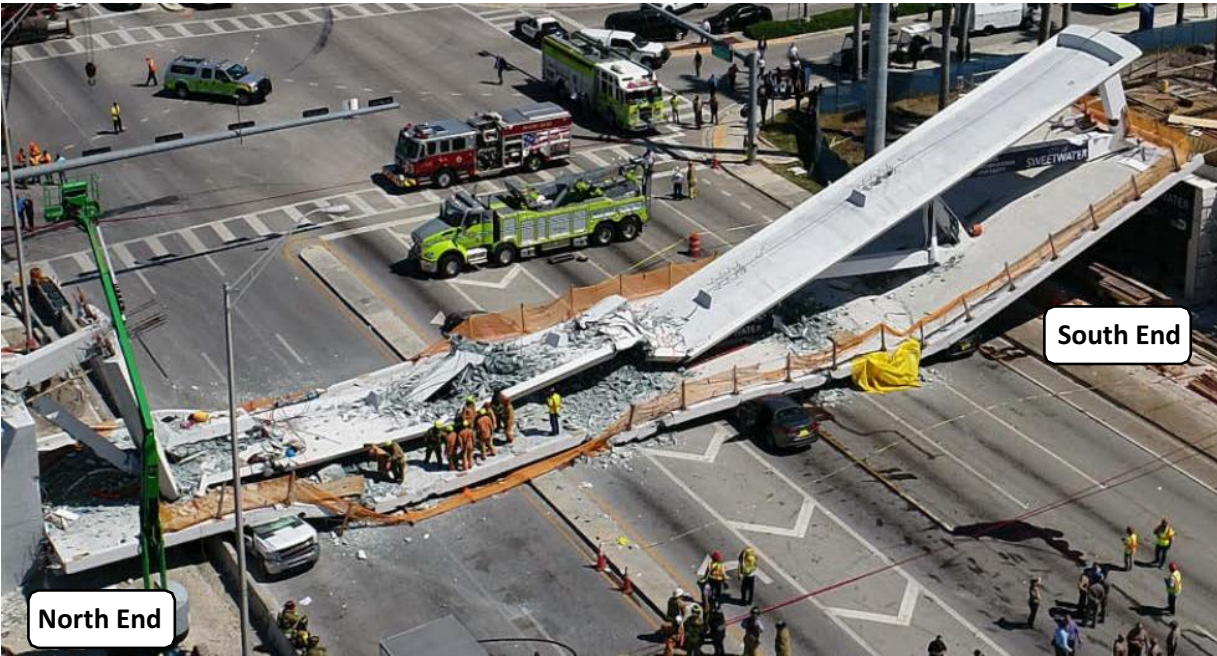


Figure 2. Aerial photograph of the FIU pedestrian bridge after collapse

SCOPE

This is a factual report that documents the evidence received by TFHRC staff, outlines the test plan for the recovered evidence, and presents the data collected from testing. The testing described herein was performed by said TFHRC staff. This report has three major sections which are based on the type of construction material tested. The three types of materials were as follows:

- concrete cores and cylinders,
- steel post-tensioning rods, and
- steel reinforcing bars.

Each section of this report includes the following information:

- documentation of the evidence received or collected,
- the testing plans for a given piece or set of evidence, and
- a presentation of the testing results.

CONCRETE CORES AND CYLINDERS

This section describes the concrete-related evidence received by FHWA-TFHRC and the test plan for concrete samples. A total of 43 concrete samples were received. Twenty-three of these samples were recovered directly from the bridge structure by means of core drilling. Fifteen samples were received from two engineering firms hired to conduct quality control testing on the concrete used in the bridge structure. Two concrete cylinder samples (in their molds) were recovered from the collapse site. The remaining three samples were pieces (chunks) of concrete recovered from the collapse site.

Documentation

The concrete-related evidence received by FHWA-TFHRC was unpacked, labeled, inspected and photographed. The following section describes the samples received along with relevant information about each sample.

Figure 3 shows the concrete core samples extracted from the bridge deck. A total of eight full or partial core segments were received. Table 1 lists the length for each specimen and relevant notes.



(a) Appearing left-to-right, Core #1 – Deck through Core #4 – Deck



(b) Appearing left-to-right, Core #5 – Deck through Core #8 – Deck

Figure 3. Concrete core samples extracted from the bridge deck

Table 1. Details of concrete core samples extracted from the bridge deck

ID	Diameter (in)	Length (in)	Usable Length [†] (in)	Notes
Core #1 – Deck	3.75	14.25	0.0	Sample had a full-depth crack along its length
Core #2 – Deck	3.75	11.0	7.12	Sample had shape deformities from coring that made a portion of the sample unusable
Core #3 – Deck	3.75	14.125	9.25	Sample had a blue, corrugated plastic tube embedded approximately 4-inch from one end running transversely
Core #4 – Deck	3.75	14.0	10.25	Sample had shape deformities from coring that made a portion of the sample unusable
Core #5 – Deck	3.75	4.25	3.0	Sample had shape deformities from coring that made a portion of the sample unusable
Core #6 – Deck	3.75	1.50	1.50	None
Core #7 – Deck	3.75	12.75	8.50	Sample had shape deformities from coring that made a portion of the sample unusable
Core #8 – Deck	3.75	9.50	8.50	Sample had shape deformities from coring that made a portion of the sample unusable

[†] Usable length as a cylindrical test specimen

Figure 4 shows the concrete core samples recovered from the canopy of the bridge. A total of five full cores or partial core segments were received. Table 2 lists the length of each specimen and relevant notes.



Figure 4. Concrete core samples extracted from the canopy of the bridge, from left-to-right, Core #1 – Canopy, #2A – Canopy, #2B – Canopy, #3 – Canopy, and #4 – Canopy

Table 2. Details of concrete core samples extracted from the canopy of the bridge

ID	Diameter (in)	Length (in)	Usable Length [†] (in)	Notes
Core #1 – Canopy	5.5	2.25	2.25	Small crack in the sample
Core #2A – Canopy	3.75	1.0	1.0	None
Core #2B – Canopy	3.75	11.5	7.125	Sample has a plastic conduit running through it in the transverse direction
Core #3 – Canopy	3.75	11.75	11.0	Sample had shape deformities from coring that made a portion of the sample unusable
Core #4 – Canopy	3.75	12.5	8.0	Sample had shape deformities from coring that made a portion of the sample unusable

[†] Usable length as a cylindrical test specimen

Figure 5 shows the concrete cylinder samples recovered from two engineering firms^a hired to conduct quality control testing on the concrete used in the bridge structure. All 15 cylinder samples shown were mold-cast with nominal dimensions of 4 inches in diameter and 8 inches in length. These samples were taken from different concrete mixtures used in different portions of the bridge structure including the deck, canopy, post-tensioning (PT) blister pockets, footings, and stairs. Three to five different concrete mixtures are represented here with specified compressive strengths between 3,000 psi and 8,500 psi. FHWA-TFHRC was provided documentation for each cylinder sample. These documents were provided by the respective engineering firms.



Figure 5. Concrete cylinder samples received from Professional Service Industries, Inc. (top) and Universal Engineering Sciences (bottom)

^a Concrete cylinder samples were recovered from Professional Service Industries, Inc. and Universal Engineering Sciences.

Figure 6 (a) and (b) show the concrete core samples recovered from what the evidence tag refers to as the “pier 2 diaphragm”. These core segments each measured 9.5 inches in diameter and varied in length. The voids left by these two core locations were used as the “pick points” during removal of a portion of the collapsed bridge structure from the roadway.



(a) Appearing left-to-right, Sample #1A through #1E



(a) Appearing left-to-right, Sample #2A through #2E

Figure 6. Pier 2 diaphragm concrete core samples

Figure 7 shows two concrete samples (left side of the figure) that were recovered at the collapse site and appear to have originally resided in the structure adjacent to the drain pipe that passed through the north diaphragm immediately under Member 12. The two samples shown on the right side of Figure 7 are associated with an evidence tag that reads “unknown pre-poured specimens.” The unknown concrete cylinder samples were delivered to FHWA-TFHRC in their molds and these molds were not removed. These samples measure 4 inches in diameter and 8 inches in height.



Figure 7. Concrete samples recovered from drain pipe region (left) and unknown concrete cylinder samples (right)

Lastly, Figure 8 shows a piece of concrete with an embedded PT duct that was recovered from the south end of the bridge structure after the collapse.



Figure 8. Concrete segment with embedded PT duct recovered from south end of bridge

Testing Plan

NTSB expressed two specific needs regarding the mechanical properties of the structural concrete that composed the bridge structure. First, there was a need to determine if the concrete used in the superstructure of the bridge meets the project specified requirements. Second, there was a need to capture the representative mechanical properties of the materials to facilitate potential computational modeling of the bridge structure or its subassemblies. Mechanical properties of interest included compressive strength, tensile strength, elastic moduli in tension and compression, Poisson's ratio, and the full compressive and tensile stress-strain response.

Compression Behavior Testing

The compressive strength of concrete was evaluated using ASTM C39^b, *Standard Test Method for Compressive Strength of Cylindrical Concrete Specimens*. Specimens were created from the concrete core samples removed from the bridge structure. Thus, ASTM C42^c, *Standard Test Method for Obtaining and Testing Drilled Cores and Sawed Beams of Concrete*, was used in conjunction with C39. Samples were tested on a 1,000-kip capacity compression machine at FHWA-TFHRC. Figure 9 shows a representative photo of the test setup for compressive behavior of concrete core samples. During testing, load was measured from the compression machine's on-board load cell.

The compressive elastic modulus and Poisson's ratio of concrete was evaluated according to ASTM C469^d, *Standard Test Method for Static Modulus of Elasticity and Poisson's Ratio of Concrete in Compression*. This testing protocol was conducted on the same cylinders that were used for compressive strength testing. During testing, compressive strain data was collected using a measuring device mounted on the specimen. This device uses three linear variable differential transformer (LVDT) displacement transducers to measure axial displacement (shown in Figure 9), which is used to calculate compressive strain. This device is otherwise referred to as an "extensometer." During testing, strain was also measured around the circumference of the sample using a circumferential strain transducer (shown in Figure 9). The axial and circumferential strains were used to determine the sample's Poisson's ratio.

The extensometer shown in Figure 9 was used in conjunction with 1,000-kip capacity compression machine's on-board load cell to capture the compressive stress-strain response of concrete.

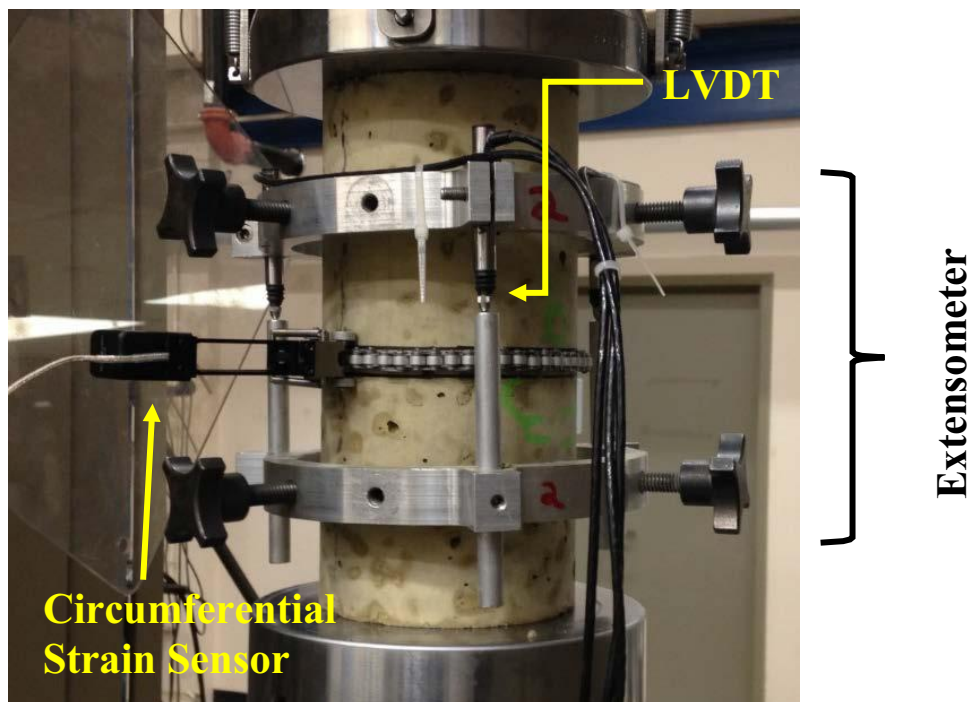


Figure 9. Test setup for compressive behavior of concrete core samples

The test matrix for determining the compressive behavior of concrete core samples is shown in Table 3. The table denotes the sample ID, details related to sample geometry, and the testing protocols; the sample ID denotes the location on the bridge from which the core sample was recovered. Prior to testing, samples were cut to length and the ends of the cores were ground flat and parallel using a cylinder end-grinder.

Table 3. Testing matrix compressive behavior of concrete core samples

ID	As-Received Core Dimensions		Measured Sample Dimensions After Cutting and Grinding			Testing Protocols
	Diameter, <i>D</i> (in)	Length, <i>L</i> (in)	Diameter [†] , <i>D</i> (in)	Length ^{††} , <i>L</i> (in)	Length-to-Diameter Ratio (<i>L/D</i>)	
Core #3 – Deck	3.75	14.13	3.72	7.52	2.02	Compressive strength (ASTM C39), Elastic Modulus and Poisson’s Ratio (ASTM C496), Compressive stress-strain behavior
Core #4 – Deck	3.75	14.00	3.72	7.51	2.02	Compressive strength (ASTM C39), Elastic Modulus and Poisson’s Ratio (ASTM C496), Compressive stress-strain behavior
Core #7 – Deck	3.75	12.75	3.72	7.46	2.01	Compressive strength (ASTM C39), Elastic Modulus and Poisson’s Ratio (ASTM C496), Compressive stress-strain behavior
Core #2B – Canopy	3.75	11.50	3.71	6.61	1.78	Compressive strength (ASTM C39), Elastic Modulus and Poisson’s Ratio (ASTM C496), Compressive stress-strain behavior
Core #3 – Canopy	3.75	11.75	3.71	6.74	1.82	Compressive strength (ASTM C39), Elastic Modulus and Poisson’s Ratio (ASTM C496), Compressive stress-strain behavior
Core #4 – Canopy	3.75	12.50	3.71	6.64	1.79	Compressive strength (ASTM C39), Elastic Modulus and Poisson’s Ratio (ASTM C496), Compressive stress-strain behavior

[†] Average of two perpendicular measurements taken at the sample’s mid-height. Measurements acquired using a digital micrometer.

^{††} Average of four measurements taken from 0°, 90°, 180°, and 270° around the sample’s perimeter. Measurements acquired using a digital micrometer.

^b ASTM C39. (2018). “*Standard Test Method for Compressive Strength of Cylindrical Concrete Specimens.*” ASTM Annual Book of Standards 04.02. ASTM International. West Conshohocken, PA.

^c ASTM C42. (2016). “*Standard Test Method for Obtaining and Testing Drilled Cores and Sawed Beams of Concrete.*” ASTM Annual Book of Standards 04.02. ASTM International. West Conshohocken, PA.

^d ASTM C469. (2014). “*Standard Test Method for Static Modulus of Elasticity and Poisson’s Ratio of Concrete in Compression.*” ASTM Annual Book of Standards 04.02. ASTM International. West Conshohocken, PA.

Tensile Behavior Testing

Figure 10 and Figure 11 show representative photos of the test setup that was used to determine tension behavior of concrete core samples.

The tensile strength of concrete cores was evaluated using U.S. Bureau of Reclamation (USBR) test method USBR 4914-92^e, *Direct Tensile Strength, Static Modulus of Elasticity, and Poisson's Ratio of Cylindrical Concrete Specimens in Tension*. Specimens were created from the concrete core samples removed from the bridge structure that conform to ASTM C42. Samples were tested on a 22-kip capacity universal testing machine at FHWA-TFHRC. During testing, load was measured from the machine's on-board load cell, and axial and circumferential strains were measured using the same type of measurement devices shown in Figure 9. The extensometer was used in conjunction with the 22-kip machine's on-board load cell to capture the tensile stress-strain response of concrete.

The test matrix used to determine the tensile behavior of concrete core samples is shown in Table 4. The table denotes the sample ID, details related to sample geometry, and the testing protocols; the sample ID denotes the location on the bridge from which the core sample was recovered. Concrete from the bridge canopy was not tested for tensile properties. Prior to testing, samples were cut to length and the ends of the cores were ground flat and parallel using a cylinder end-grinder.

^e USBR 4914-92. "Procedure for Direct Tensile Strength, Static Modulus of Elasticity, and Poisson's Ratio of Cylindrical Concrete Specimens in Tension." U.S. Bureau of Reclamation, Concrete Manual Part 2, 9th edition, 1992.

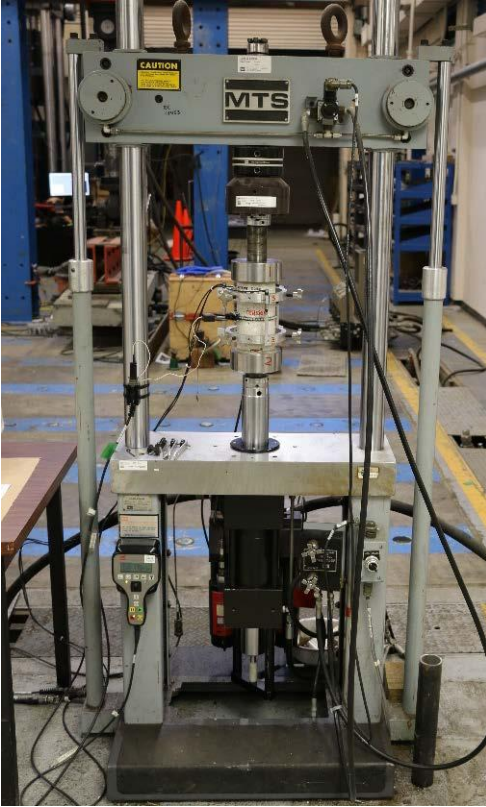


Figure 10. Concrete tension testing machine



Figure 11. Close-up view of concrete tension test sample in the test machine

Table 4. Testing matrix tensile behavior of concrete core samples

ID	As-Received Core Dimensions		Measured Sample Dimensions After Cutting and Grinding			Testing Protocols
	Diameter, D (in)	Length, L (in)	Diameter [†] , D (in)	Length ^{††} , L (in)	Length-to-Diameter Ratio (L/D)	
Core #2 – Deck	3.75	11.00	3.72	6.89	1.85	Tensile strength, Elastic Modulus and Poisson’s Ratio, Tensile stress-strain behavior (USBR 4914-92)
Core #8 – Deck	3.75	9.50	3.72	6.89	1.85	Tensile strength, Elastic Modulus and Poisson’s Ratio, Tensile stress-strain behavior (USBR 4914-92)

[†] Average of two perpendicular measurements taken at the sample’s mid-height. Measurements acquired using a digital micrometer.

^{††} Average of four measurements taken from 0°, 90°, 180°, and 270° around the sample’s perimeter. Measurements acquired using a digital micrometer.

Air, Aggregate, and Paste Contents of Concrete

The constituents of the hardened concrete were determined by petrographic assessment. This assessment was pursued to determine whether the concrete in the bridge structure conformed to the intended mix design and specification requirements. This assessment was conducted according to ASTM C457^f, *Standard Test Method for Microscopical Determination of Parameters of the Air-Void System in Hardened Concrete*. The results of this test include air, aggregate, and paste contents of the hardened concrete. To execute this test, sample areas were cut from the six core samples listed in Table 5. Samples were cut to avoid portions of the concrete that represented near surface regions. Near surface regions (i.e., concrete that was near a finished surface) tend to exhibit different constituent proportions than those from the interior of the element.

Cut samples were lapped and polished prior to assessment. Samples were examined using a stereomicroscope^g before running the air void assessment to check for unusual surface features. Air void assessment was conducted in accordance with Procedure B of ASTM C457, which is the *Modified Point Count Method*. This test was run using a commercially available air void assessment equipment, which is shown in Figure 12.

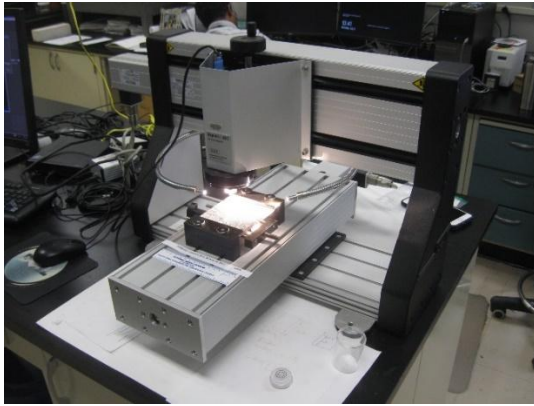
Table 5. Testing matrix for air, aggregate, and paste contents of concrete

Sample ID	Original Dimensions		Final Sample Dimensions		
	Cylinder Diameter (in)	Length (in)	Width (in)	Length (in)	Area Analyzed (in ²)
Core #1 – Deck	3.75	14.25	3.7	4.4	16.3
Core #4 – Deck	3.75	6.5 [†]	3.7	4.6	17.0
Core #5 – Deck	3.75	4.25	3.7	4.1	15.2
Core #1 – Canopy	5.5	2.25	2.8	5.5	15.4
Core #3 – Canopy	3.75	5.0 [†]	3.7	4.4	16.3
Core #4 – Canopy	3.75	5.5 [†]	3.7	4.4	16.3

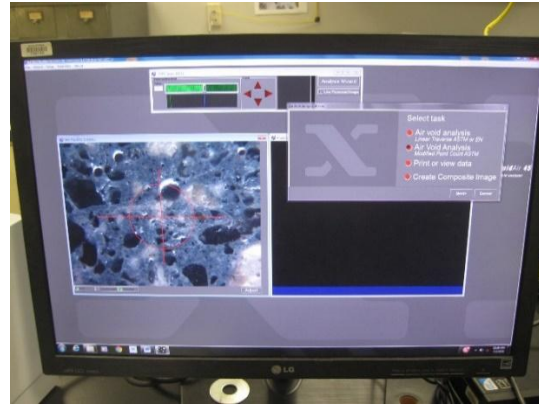
[†] Approximate length of core segment remaining after creating compression sample listed in Table 3.

^f ASTM C457. (2016). “*Standard Test Method for Microscopical Determination of Parameters of the Air-Void System in Hardened Concrete*.” ASTM Annual Book of Standards 04.02. ASTM International. West Conshohocken, PA.

^g A stereomicroscope is an optical, binocular microscope that allows for a three-dimensional visualization of the viewed object.



(a) Sample loaded into test fixture



(b) User-interface for data collection

Figure 12. Rapid Air 457 air void assessment equipment

Results

The concrete-related test results for compression behavior, tension behavior, and air, aggregate, and paste content are presented in the subsequent sections.

Compression Behavior

Table 6 summarizes the compression test results for core samples removed from the bridge deck. The table reflects each sample's average diameter, average length, unit weight, compressive strength, axial strain at peak compressive stress, elastic modulus, and Poisson's ratio. The sample diameter was determined by averaging two perpendicular measurements taken at the sample's mid-height. The sample length was determined by averaging four measurements taken from 0°, 90°, 180°, and 270° around the sample's perimeter. Both length and diameter measurements were acquired using a digital micrometer. The unit weight was determined by dividing the sample weight by the average sample volume which was calculated using the average diameter and length. The compressive strength is defined as the stress that occurs at the peak compressive load. As previously noted, each sample was instrumented with an extensometer that captured axial deformation at the mid-height of the sample over a 4-inch gauge length. Deformation was recorded using a set of three LVDTs whose results were averaged. Axial strain was calculated by dividing this average deformation by the gauge length.

The elastic modulus was determined by calculating the slope of the compressive stress-strain curve between compressive stress values of 0.85 ksi and 3.4 ksi; these stress limits correspond to 10% and 40% of the specified compressive strength, $f'_{c,spec}$, of the concrete, which was 8.5 ksi. The Poisson's ratio was determined by calculating the slope of the circumferential strain (plotted on the y-axis) versus axial compressive strain curve (plotted on the x-axis) within a compressive stress range between 2.5 ksi and 3.4 ksi. This data range differs from that prescribed by ASTM C469. The measured circumferential strains exhibited non-linear behavior between stresses of 0 ksi and 2.5 ksi but appeared linear thereafter; thus, the range over which Poisson's ratio was calculated was modified to account for non-linearity in the data. The non-linearities in the data are attributed to the device used to measure the circumferential strain.

ASTM C469 specifies that the samples shall be loaded and unload three times. The elastic modulus and Poisson's ratio data reported in Table 6 reflects the average of these three cycles. The elastic modulus and Poisson's ratio measurement ranges and the aforementioned cycles can be observed in Figure 13.

Figure 13 depicts the compressive stress-strain response of the three bridge deck core samples tested. A circular marker has been added to each curve to identify the peak compressive stress. The curves were truncated immediately prior to abrupt loss of load carrying capacity due to concrete crushing.

Figure 14 presents representative images of bridge deck core samples after compression testing. All three samples exhibited compression failure, and the failure type according to ASTM C39 is listed in Table 6.

Table 6. Summary of compression testing results for bridge deck core samples

Sample ID	Core #3 - Deck	Core #4 - Deck	Core #7 - Deck
Average Diameter (in)	3.72	3.72	3.72
Average Length (in)	7.52	7.51	7.46
Unit Weight (lb/ft ³)	137.9	138.8	138.7
Compressive Strength (ksi)	8.58	10.09	10.77
Axial Strain at Peak Compressive Stress	0.0022	0.0026	0.0028
Elastic Modulus (Average of 3 Cycles) (ksi)	4408	4707	4639
Poisson's Ratio (Average of 3 Cycles)	0.133	0.183	0.151
Failure Type per ASTM C39	Type 1	Type 1	Type 1

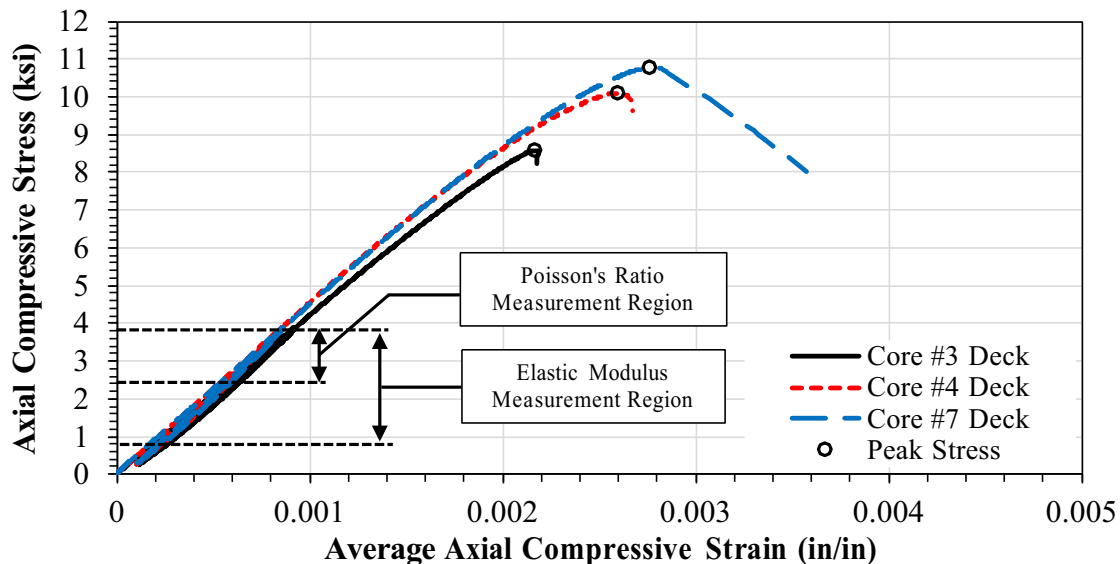


Figure 13. Compressive stress-strain relationships for bridge deck core samples



(a) Concrete Core #3 – Deck: Front



(b) Concrete Core #3 – Deck: Back



(c) Concrete Core #4 – Deck: Front



(d) Concrete Core #4 – Deck: Back



(e) Concrete Core #7 – Deck: Front



(f) Concrete Core #7 – Deck: Back

Figure 14. Photographs of bridge deck core samples after compression testing

Table 7 summarizes the compression test results for core samples removed from the bridge canopy. The table reflects each sample's average diameter, average length, unit weight, compressive strength, axial strain at peak compressive stress, elastic modulus, and Poisson's ratio. These results were determined using the same methods described previously for the results shown in Table 6.

Figure 15 depicts the compressive stress-strain response of the three bridge canopy core samples tested. A circular marker has been added to each curve to identify the peak compressive stress. The curves were truncated immediately prior to abrupt loss of load carrying capacity due to concrete crushing.

Figure 16 presents representative images of bridge canopy core samples after compression testing. All three samples exhibited compression failure, and the failure type according to ASTM C39 is listed in Table 7.

Table 7. Summary of compression testing results for bridge canopy core samples

Sample ID	Core #2B - Canopy	Core #3 - Canopy	Core #4 - Canopy
Average Diameter (in)	3.71	3.71	3.71
Average Length (in)	6.61	6.74	6.64
Unit Weight (lb/ft ³)	139.0	139.9	138.8
Compressive Strength (ksi)	10.34	10.74	10.42
Axial Strain at Peak Compressive Stress	0.0027	0.0027	0.0028
Elastic Modulus (Average of 3 Cycles) (ksi)	4430	4784	4536
Poisson's Ratio (Average of 3 Cycles)	0.126	0.112	0.130
Failure Type per ASTM C39	Type 3	Type 1	Type 3

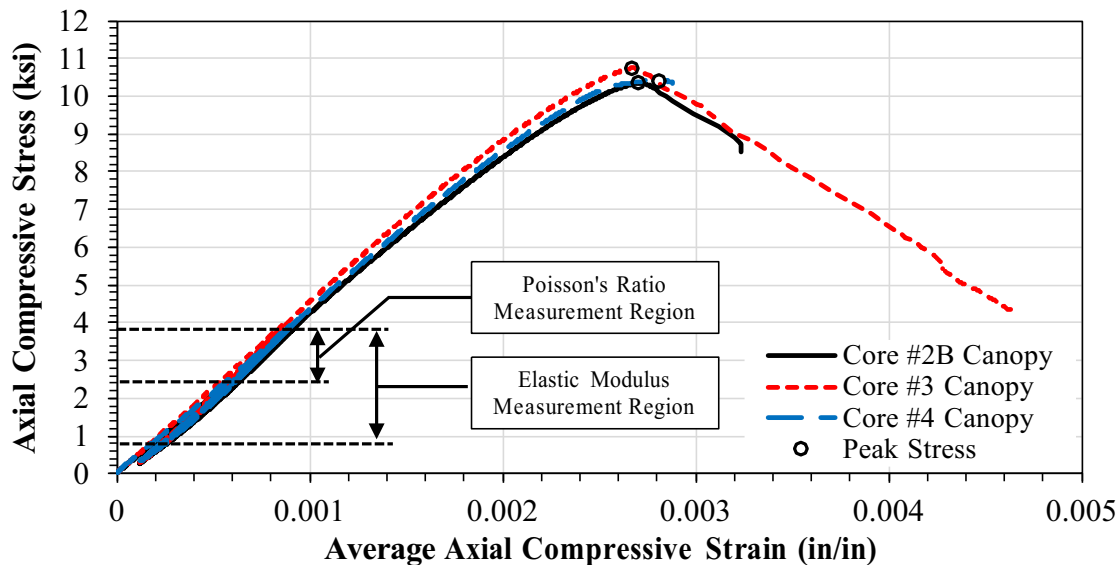


Figure 15. Compressive stress-strain relationships for bridge canopy core samples



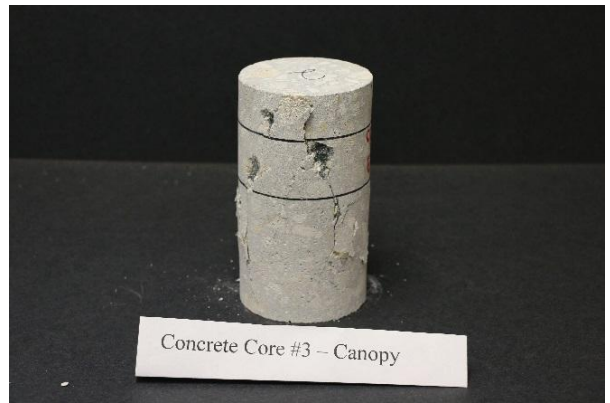
(a) Concrete Core #2B – Canopy: Front



(b) Concrete Core #2B – Canopy: Back



(c) Concrete Core #3 – Canopy: Front



(d) Concrete Core #3 – Canopy: Back



(e) Concrete Core #4 – Canopy: Front



(f) Concrete Core #4 – Canopy: Back

Figure 16. Photographs of bridge canopy core samples after compression testing

Tension Testing

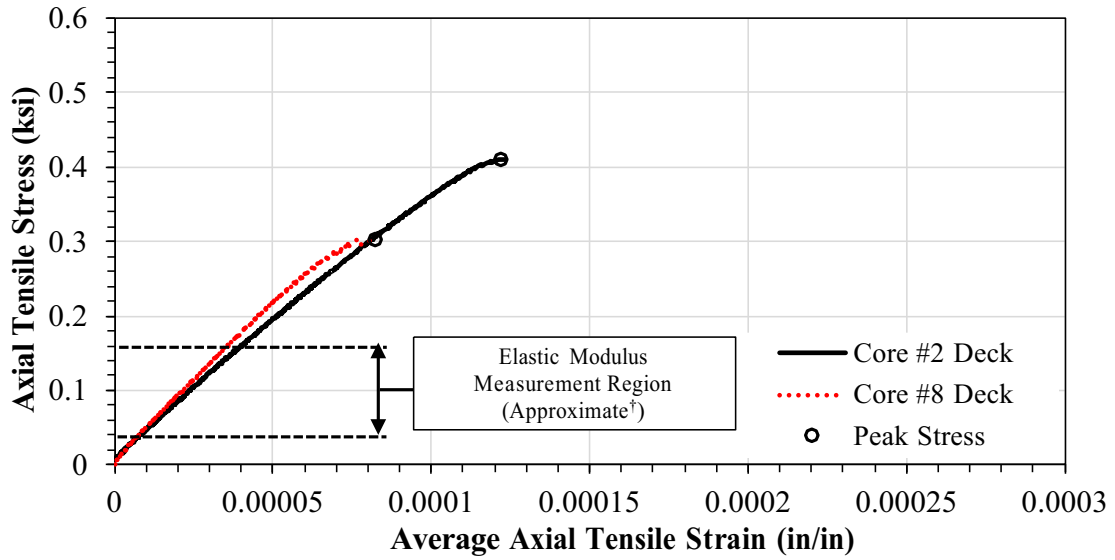
Table 8 summarizes the tension test results for core samples removed from the bridge deck. The table reflects each sample's average diameter, average length, unit weight, tensile strength, axial strain at peak tensile stress, and elastic modulus. The sample diameter was determined by averaging two perpendicular measurements taken at the sample's mid-height. The sample length was determined by averaging four measurements taken from 0°, 90°, 180°, and 270° around the sample's perimeter. Both length and diameter measurements were acquired using a digital micrometer. The unit weight was determined by dividing the sample weight by the average sample volume which was calculated using at the average diameter and length. The tensile strength is defined as the stress that occurs at the peak tensile load. As previously noted, each sample was instrumented with an extensometer that captured axial deformation at the mid-height of the sample over a 4-inch gauge length. Deformation was recorded using a set of three LVDTs which were averaged. Axial strain was calculated by dividing this average deformation by the gauge length. The elastic modulus was determined by calculating the slope of the tensile stress-strain response between 10% and 40% of the measured tensile strength. This range is approximately shown in Figure 17. The magnitude of the strains recorded by the circumferential strain sensor were outside of device's resolution, and therefore they were not reliable. Hence, Poisson's ratio has not been reported.

Figure 17 depicts the tensile stress-strain response of the two bridge deck core samples tested in tension. A circular marker has been added to each curve to identify the peak tensile stress. The curves were truncated immediately prior to abrupt loss of load carrying capacity due to tensile rupture of concrete.

Figure 18 presents representative images of bridge deck core samples after tension testing. Both samples failed by tensile rupture of concrete within the 4-inch extensometer gauge length. The fracture surface was normal to the direction of loading, which is expected for a brittle material that fails in principal tension.

Table 8. Summary of tension testing results for bridge deck core samples

Sample ID	Core #3 - Deck	Core #4 - Deck
Average Diameter (in)	3.72	3.72
Average Length (in)	6.89	6.89
Unit Weight (lb/ft ³)	138.0	139.3
Tensile Strength (ksi)	0.41	0.30
Axial Strain at Peak Tensile Stress	0.00012	0.00008
Elastic Modulus (ksi)	3758	4285



† The elastic modulus was determined by calculating the slope of the tensile stress-strain curve between 10% and 40% of the measured tensile strength, thus the displayed range is approximate.

Figure 17. Tensile stress-strain relationships for bridge deck core samples



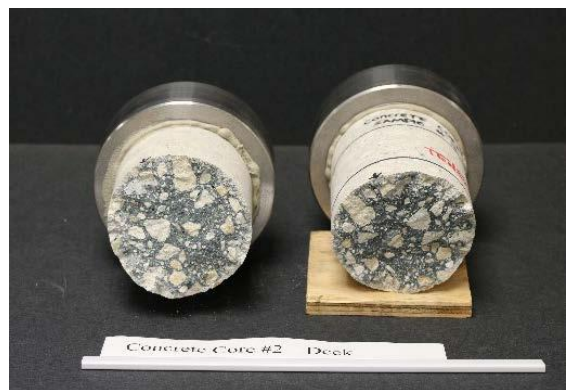
(a) Fracture location



(b) Fracture surface



(a) Fracture location



(b) Fracture surface

Figure 18. Photographs of bridge deck core samples after tension testing

Air, Aggregate, and Paste Content

Six concrete core samples extracted from the bridge structure were tested for air, aggregate, and paste contents. The results from this assessment are listed in Table 9 and Table 10 for concrete cores recovered from the bridge deck and canopy, respectively. ASTM C457 refers to ASTM C125^h *Standard Terminology Relating to Concrete and Concrete Aggregate* for definition of terms. Entrained air voids are defined to typically be between 10 µm and 1000 µm (1 mm) in diameter and spherical or nearly so, that are incorporated intentionally into a cementitious mixture during mixing by use of an air entraining admixture. Entrapped air voids are defined to typically be 1 mm or larger in size and mainly irregular in shape that are incorporated unintentionally into a cementitious mixture during mixing and handling. The point count results reflected in Table 9 and Table 10 were performed on a minimum surface area of 12 square inches for the prepared surfaces. This is the minimum specified area for a concrete with a nominal maximum coarse aggregate size of 1 inch.

Table 9. Point-count results from samples recovered from the deck of the bridge structure

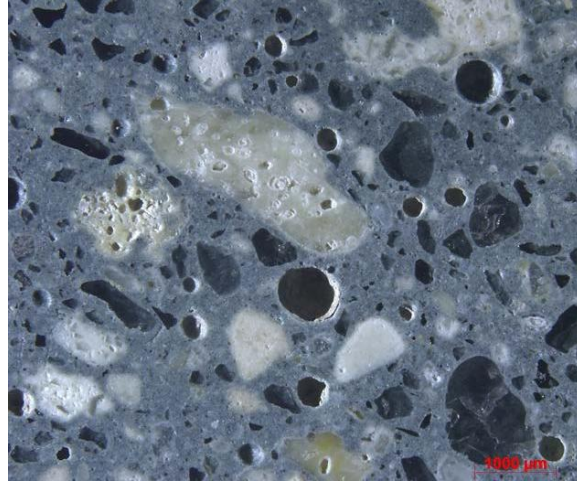
Sample ID	Air Content (%)			Paste Content (%)	Aggregate Content (%)
	Entrained	Entrapped	Total		
Core #1 - Deck	2.0	0.3	2.3	33.9	63.8
Core #4 - Deck	1.7	0.0	1.7	37.6	60.7
Core #5 - Deck	4.0	0.4	4.4	33.2	62.4

Table 10. Point-count results from samples recovered from the canopy of the bridge structure

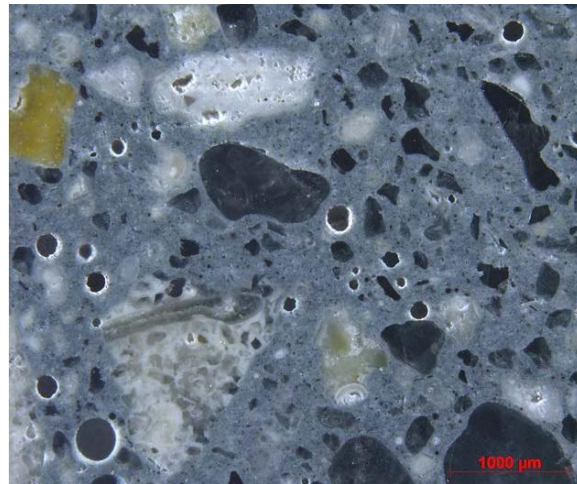
Sample ID	Air Content (%)			Paste Content (%)	Aggregate Content (%)
	Entrained	Entrapped	Total		
Core #1 - Canopy	2.0	0.7	2.7	32.3	65.0
Core #3 - Canopy	4.4	0.1	4.5	34.8	60.7
Core #4 - Canopy	4.5	0.0	4.5	33.1	62.4

Figure 19 shows representative stereomicroscope images of representative petrographic assessment samples of deck concrete. The cementitious paste in these samples was dominantly dark greenish gray. The coarse aggregate was found to be fossiliferous limestone, and the fine aggregate was found to be a limestone and siliceous sand. The black circular objects are air voids. The scale is shown in the lower right corner of each image.

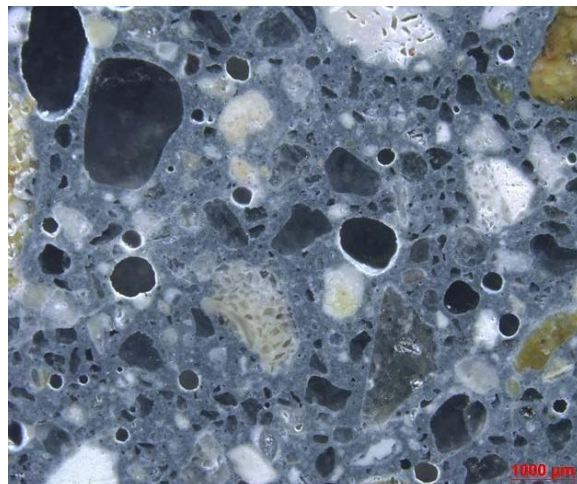
^h ASTM C125. (2018). “*Standard Terminology Relating to Concrete and Concrete Aggregate*.” ASTM International. West Conshohocken, PA.



(a) Core #1 - Deck



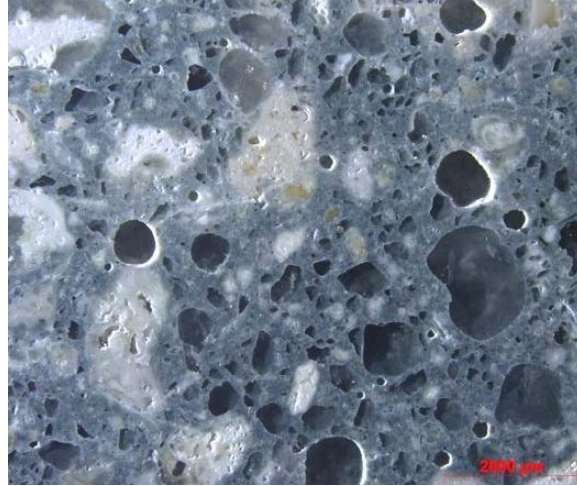
(b) Core #4 - Deck



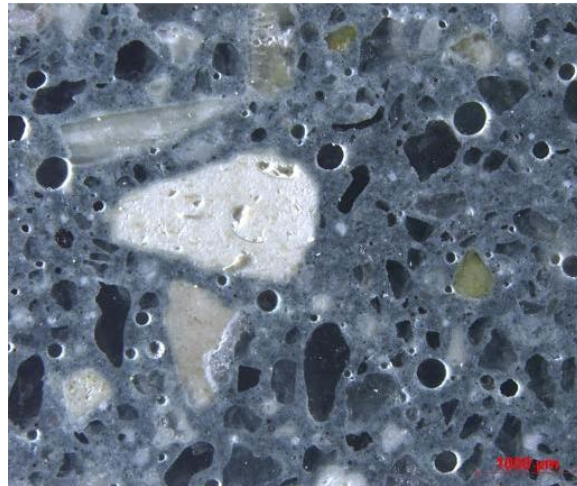
(c) Core #5 - Deck

Figure 19. Stereomicroscope photomicrographs of representative petrographic assessment samples of deck concrete

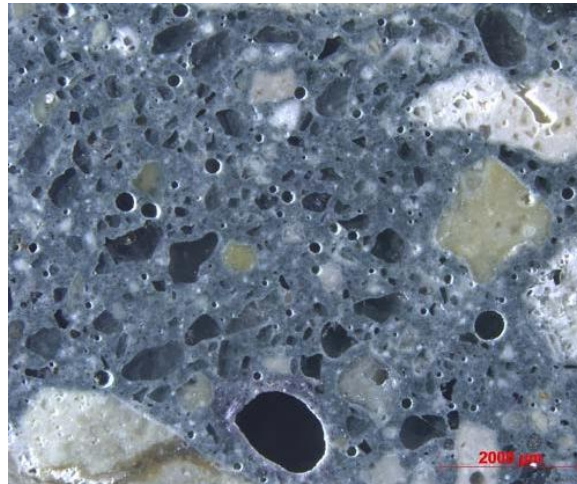
Figure 20 shows representative stereomicroscope images of representative petrographic assessment samples of canopy concrete. The cementitious paste in these samples was dominantly dark greenish gray. The coarse aggregate was found to be fossiliferous limestone, and the fine aggregate was found to be a limestone and siliceous sand. The black circular objects are air voids.



(a) Core #1 - Canopy



(b) Core #3 - Canopy



(c) Core #4 - Canopy

Figure 20. Stereomicroscope photomicrographs of representative petrographic assessment samples of canopy concrete

POST-TENSIONING RODS

This section describes the post-tensioning evidence that was received and a description of the tests performed. Two rods were received; one referred to as the virginⁱ rod, and the second from Diagonal 11 in the bridge. The Diagonal 11 rod was the rod that was being tensioned or recently had been tensioned in the moments immediately prior to the bridge collapse. The rods were 1-3/4 inch Williams All-Thread-Bar^j furnished to the requirements of ASTM A722^k.

Documentation

Figure 21 shows a picture of the two rods side-by-side. Two measuring tapes are shown for scale. The virgin rod is straight and is shown in the upper portion of Figure 21. As received, the Diagonal 11 rod is deformed into a S-shape, and is shown in the lower portion of Figure 21. An orange string has been laid near the Diagonal 11 rod to provide visual perception to the deformation. The measured dimensions of each rod are shown in Figure 22. The lateral plastic deformation of the Diagonal 11 rod is assumed to have occurred during the collapse. There was approximately 36 inches of what appears to be straight, non-plastically deformed rod on the left end of the Diagonal 11 rod as shown in Figure 21 and Figure 22.

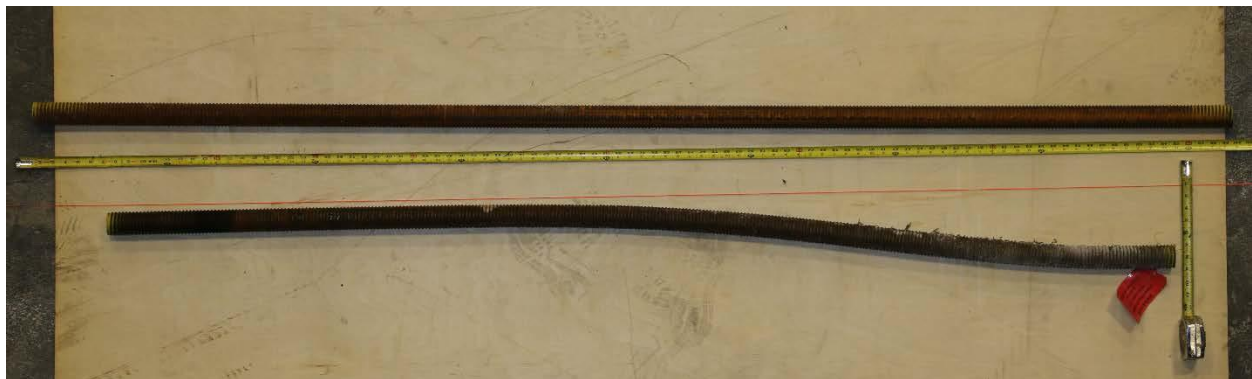
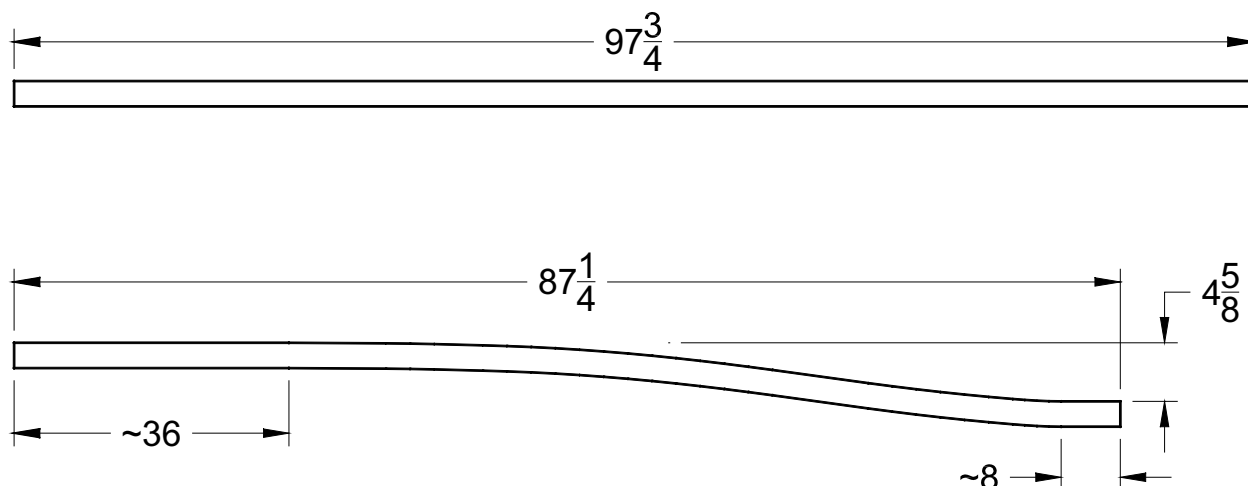


Figure 21. Picture of virgin rod (top) and Diagonal 11 rod (bottom)

ⁱ A virgin post-tensioning rod is a rod that had not yet been installed in the structure and thus had not been subjected to structural loading/unloading during bridge construction nor the subsequent collapse of the bridge. The virgin rod was obtained from a stockpile of post-tensioning rods that were at the bridge site awaiting installation in later portions of the bridge.

^j © Williams Form Engineering Corp. of Belmont, MI.

^k ASTM A722. (2015). "Standard Specification for High-Strength Steel Bars for Prestressed Concrete." ASTM Annual Book of Standards 01.04. ASTM International. West Conshohocken, PA



Note: Units in inches.

Figure 22. Dimensions of virgin rod (top) and Diagonal 11 rod (bottom)

Test Plan

NTSB expressed two specific needs in terms of the mechanical properties of post-tensioning rods. First, there was a need to confirm conformance of the rods to their specification. Second, there was a need to capture accurate stress versus strain behavior in order to facilitate potential modeling of the global and local performance of the structure.

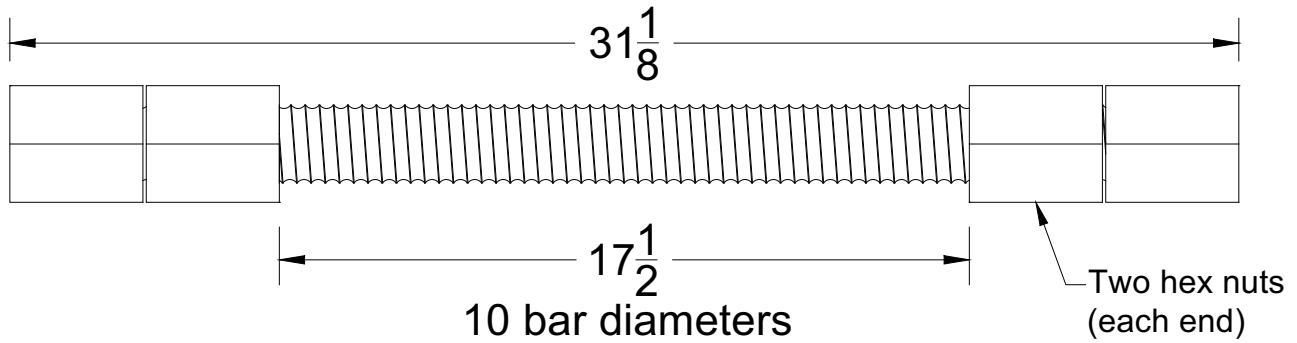
ASTM A722 defines the following requirements:

- a minimum tensile strength of 150 ksi,
- a minimum yield strength of 120 ksi,
- a minimum elongation of 4% or 7% depending if the gauge length is 20 or 10 bar diameters, respectively,
- tensile testing shall be performed according to ASTM A370¹, and
- phosphorous shall not exceed 0.040% and sulfur shall not exceed 0.050%.

Two specimen types were used; one tested the rod full-scale (shown in Figure 23) and a second that tested an ASTM A370 standard round bar tension coupon machined from a full-size bar (shown in Figure 24). The full-size specimen represents how the rods would normally be tested for conformance with project specifications. However, the required specimen length is approximately 31 inches. The received Diagonal 11 rod could only accommodate one of these specimens within the portion of the rod that was geometrically linear. Tension testing of the

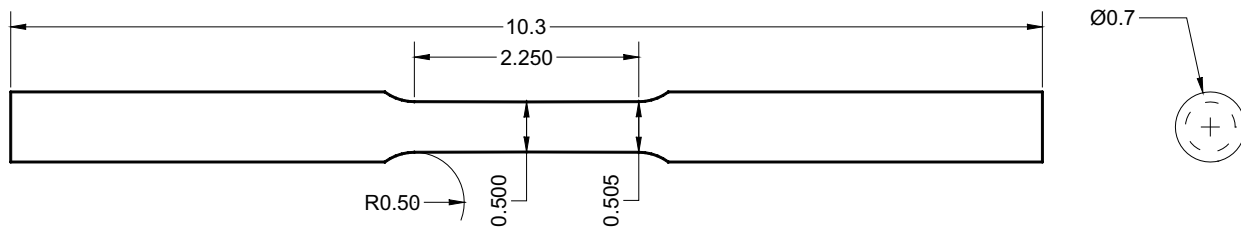
¹ ASTM A370. (2017). "Standard Test Methods and Definitions for Mechanical Testing of Steel Products." ASTM Annual Book of Standards 01.03. ASTM International. West Conshohocken, PA.

continuously threaded rod would deliver a load-deformation relationship for the rod, though NTSB expressed a need to obtain the stress versus strain response of the material. Given that the cross-section of the rod is not constant, calculating the stress versus strain relationship from the load versus displacement results was not considered to be appropriate. In terms of obtaining accurate stress versus strain curves, machining the rod to create standard round tension coupon specimens was the preferred approach since the cross-section is precisely machined.



Note: Units in inches.

Figure 23. Full-size tension specimen



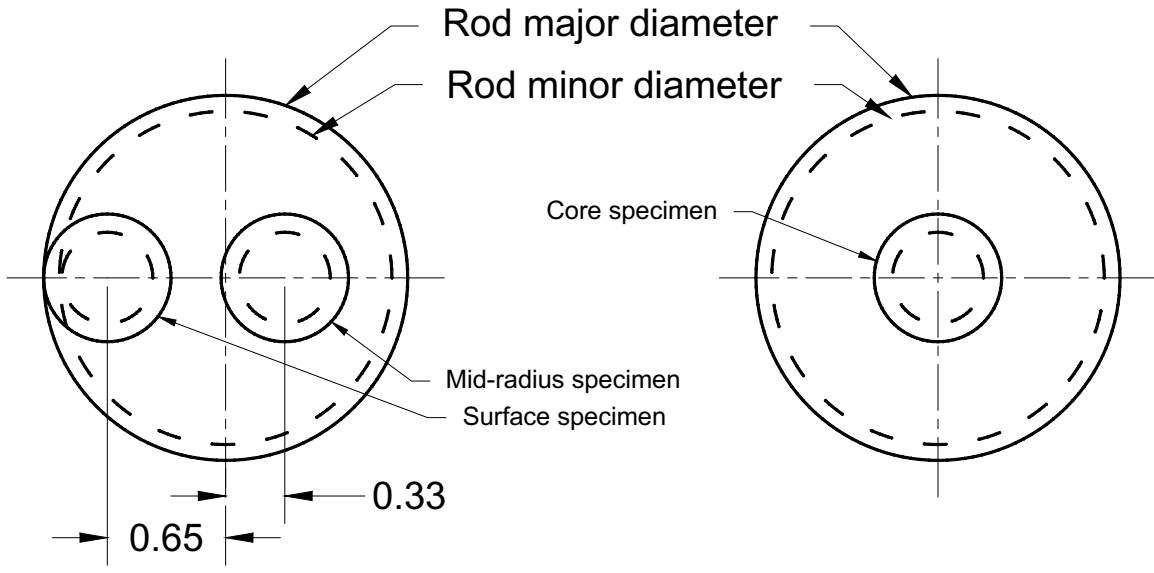
Note: Units in inches.

Figure 24. ASTM A370 standard round bar tension specimen

Using a standard round tension coupon introduces added complexity because the rods are a quenched and tempered product which may not be through-hardened. This means that the strength of the steel could be lesser in the core of the rod and greater toward the surface. Therefore, the rod was sampled at three locations through the radius of the rod to capture any radial changes to the stress versus strain properties. This is shown in Figure 25 where one sample was taken as close to the surface as possible, one at the mid-radius, and the third at the core. To supplement this further, Rockwell C hardness was assessed across the cross-section of the rod to further characterize the variability of strength across the radius. Hardness measurements were conducted in accordance with ASTM E18^m. The pattern for hardness testing is shown in Figure 26 where a slice of each rod was sampled with 65 points distributed in a polar coordinate system centered at the core of the rod. Via this point distribution, eight hardness values were captured

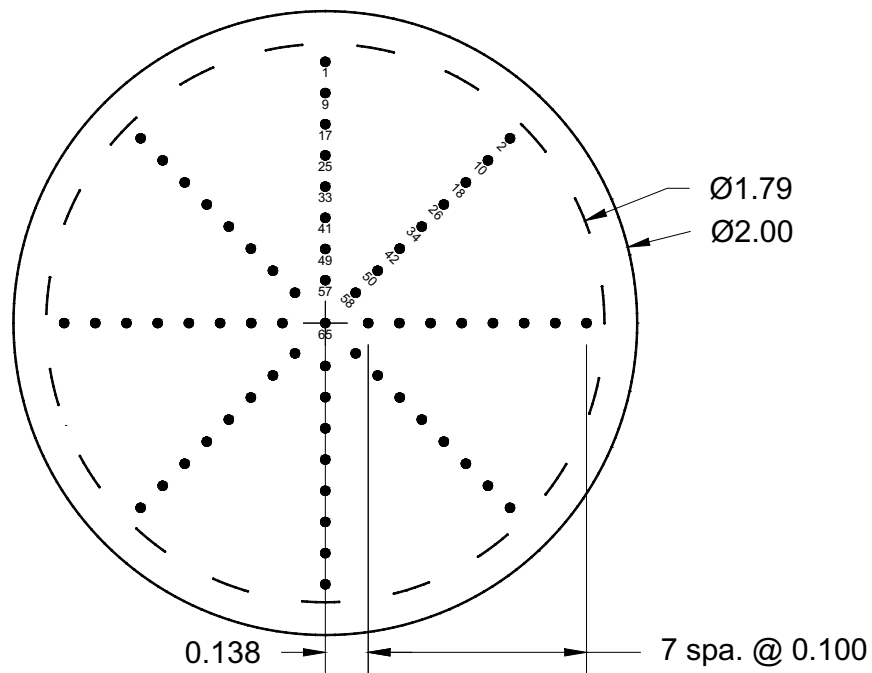
^m ASTM E18. (2017). “Standard Test Methods for Rockwell Hardness of Metallic Materials.” ASTM Annual Book of Standards 03.01. ASTM International. West Conshohocken, PA.

and averaged at eight radial locations. This allowed for a higher fidelity assessment of through-hardening than the three sampling locations from the machine round bar specimens.



Note: Units in inches.

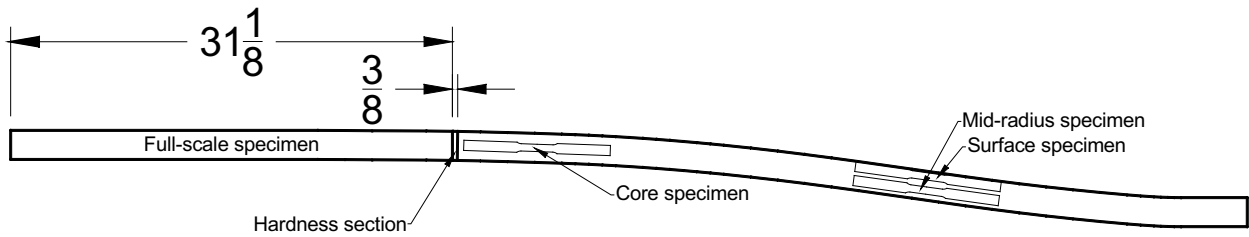
Figure 25. Radial sampling locations of round bar specimens



Note: Units in inches.

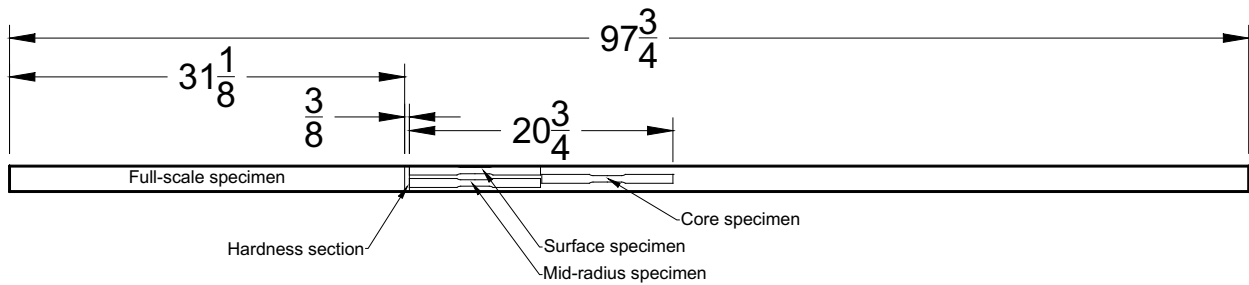
Figure 26. Radial sampling locations of round bar specimens

The actual sampling locations for the three specimen types for the Diagonal 11 rod is shown in Figure 27. The more important tension test is the full-scale specimen that was completed on the one straight portion of the rod. The smaller round bar tension specimens were fabricated from the remaining portion of the rod focusing on areas that appear to have been subjected to minimal plastic deformation. The hardness specimen was cut just to the right of the full-scale specimen. The sampling locations for the virgin rod are shown in Figure 28. On this rod, all sampling started from one end of the rod and progress along its length.



Note: Units in inches.

Figure 27. Specimen locations on Diagonal 11 rod



Note: Units in inches.

Figure 28. Specimen locations on virgin rod

Tension Test Method Description

The tension testing was conducted in a 220-kip and a 550-kip servovalve controlled hydraulic test frame, respectively shown in Figure 29 and Figure 30. Each frame was fitted with side-loading hydraulic wedge grips for gripping onto specimens. Each frame was controlled by a dedicated controller and computer that also collected data throughout the testing.



Figure 29. 220-kip test frame



Figure 30. 550-kip test frame

The same loading program was used for both machines, and thus for each of the two specimen types. The program requires the user to enter the specimen “reduced length” as it is used to determine the loading rate. The reduced length of the machined round bar specimens was 2.25-inch as shown in Figure 24. For the full-size bar specimens, it was the distance between the nut faces of the specimen after installation, and this was documented for each specimen. A high-level description of the loading program is as follows:

1. The user enters the reduced length of the specimen.
2. The initial loading rate is set at 0.015 in./min. per inch of reduced length.
3. At an axial strain of 0.015, the loading rate increases to 0.016 in./min. per inch of reduced length.
4. At an axial strain of 0.020, the loading rate increases to 0.021 in./min. per inch of reduced length.
5. At an axial strain of 0.025, the loading rate increases to 0.032 in./min. per inch of reduced length.
6. At an axial strain of 0.030, the loading rate increases to 0.055 in./min. per inch of reduced length.
7. At an axial strain of 0.035, the loading rate increases to 0.109 in./min. per inch of reduced length. This loading rate does not change for the remainder of the test.

For determining yield strength, ASTM A370 requires the displacement rate to be between $1/160$ and $1/16$ in./min. per inch of reduced length in the specimen. For determining tensile strength, ASTM A370 requires the displacement rate to be between $1/20$ and $1/2$ in./min. per inch of reduced length in the specimen. Therefore, the loading program fits within and is on the slower end of the ASTM A370 load rate ranges.

Gauge length elongation of the machined round bar specimens was measured with a clip-on extensometer with a 2.000-inch gauge length and a 1-inch range. The clip-on extensometer remained on the specimen through fracture. For the full-size rod, a video extensometer was used to monitor elongation. This device operates on the principle of digital image correlation. The specimen was painted with white spray paint, then speckled with black spray paint. The video camera is able to track the motion of this high-contrast pattern in terms of image pixels, and through calibration, pixels are converted to specimen displacements. The video extensometer was set to report elongation over a 17.5-inch long gauge length, which equates to the 10-bar diameter requirement from ASTM A722.

Tension Testing Results

The plots of the stress versus strain results for the machined round bar specimens are shown in Figure 31 and Figure 32, respectively for the three specimens from the virgin bar and the Diagonal 11 bar. The specimen labels start with “V” if it came from the virgin bar, or “11” if it came from the diagonal 11 bar. The second letter determines the radial location the specimen was machined from; “C” for the bar core, “M” from the mid-radius, and “S” from the surface. The reportable quantities for each of the machined round bar specimens are reported in Table 11. Yield strength was determined from the 0.2% offset method outlined in ASTM A370, the tensile strength is the maximum stress attained in the test, the elongation at fracture is last strain measured before significant load drop, and the reduction in area is based on the final measured diameter at the fracture.

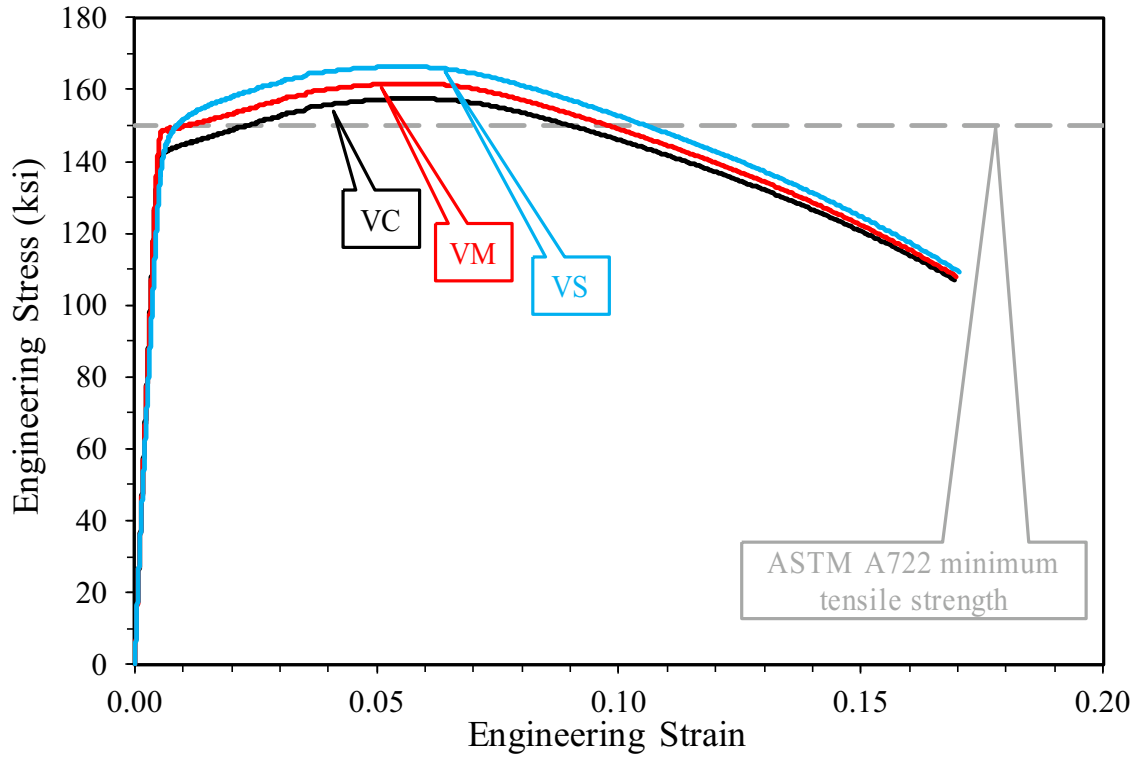


Figure 31. Stress versus strain results for virgin bar machined round specimens

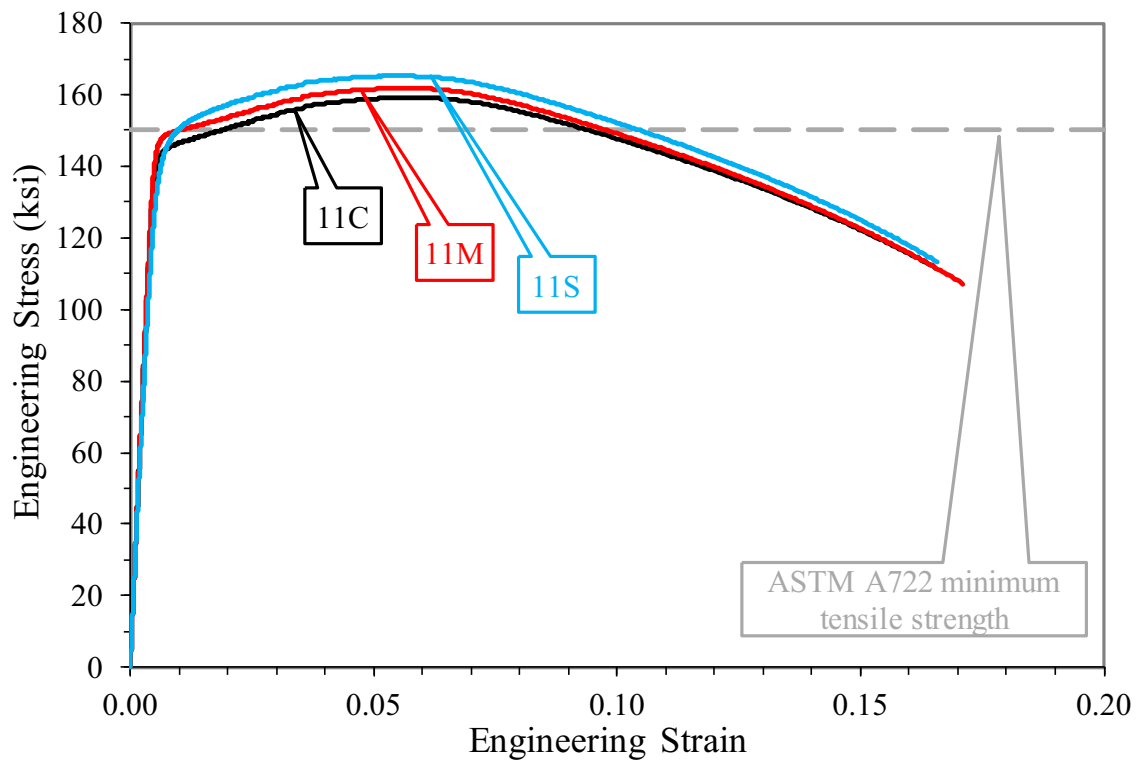


Figure 32. Stress versus strain results for diagonal 11 bar machined round specimens

Table 11. Summary results of machined round bar specimens

Specimen	Yield Strength (ksi)	Tensile Strength (ksi)	Elongation at Fracture (percent)	Reduction in Area (percent)
VC	142.8	157.5	16.9	34
VM	148.9	161.7	17.0	33
VS	147.0	166.4	17.0	34
11C	144.0	159.1	16.6	34
11M	148.3	161.8	17.1	34
11S	143.7	165.2	16.8	33
ASTM A722	≥ 120	≥ 150	≥ 7	—

— No requirement.

When the full-size bars were installed in the 550-kip machine, top and bottom nuts were spaced 19.4-inches and 19.0-inches apart, respectively for the Diagonal 11 and virgin bar, which defined the reduced length of the bar. Tabular results of the two full-size bars are presented in Table 12, and graphical results are presented in Figure 33 and Figure 34. The cross-sectional area of the bar was not measured, rather the minimum value of 2.60 in² reported by bar manufacturer is used to calculate stress. The 0.2% offset method was used to determine the yield strength. The graph in Figure 33 shows load and stress on the two vertical axes. It can be observed in this graph that the bars fractured at elongations greater than 9% and at tensile strengths greater than 150 ksi. The graph in Figure 34 plots the load versus elongation of the bars; this may be useful for defining nonlinear material properties of the post-tensioning rods in analytical models. The photos in Figure 35 and Figure 36 show the Diagonal 11 and virgin bars, respectively, after being removed from the test machine. Both specimens fractured within the 17.5-inch gauge length, thus both tests are considered valid.

Table 12. Summary results of full-size bar specimens

Specimen	Yield Strength (ksi)	Tensile Strength (ksi)	Elongation at Fracture (percent)
Diagonal 11	135.0	161.1	9.86
Virgin	136.0	161.2	9.91
ASTM A722	≥ 120	≥ 150	≥ 7

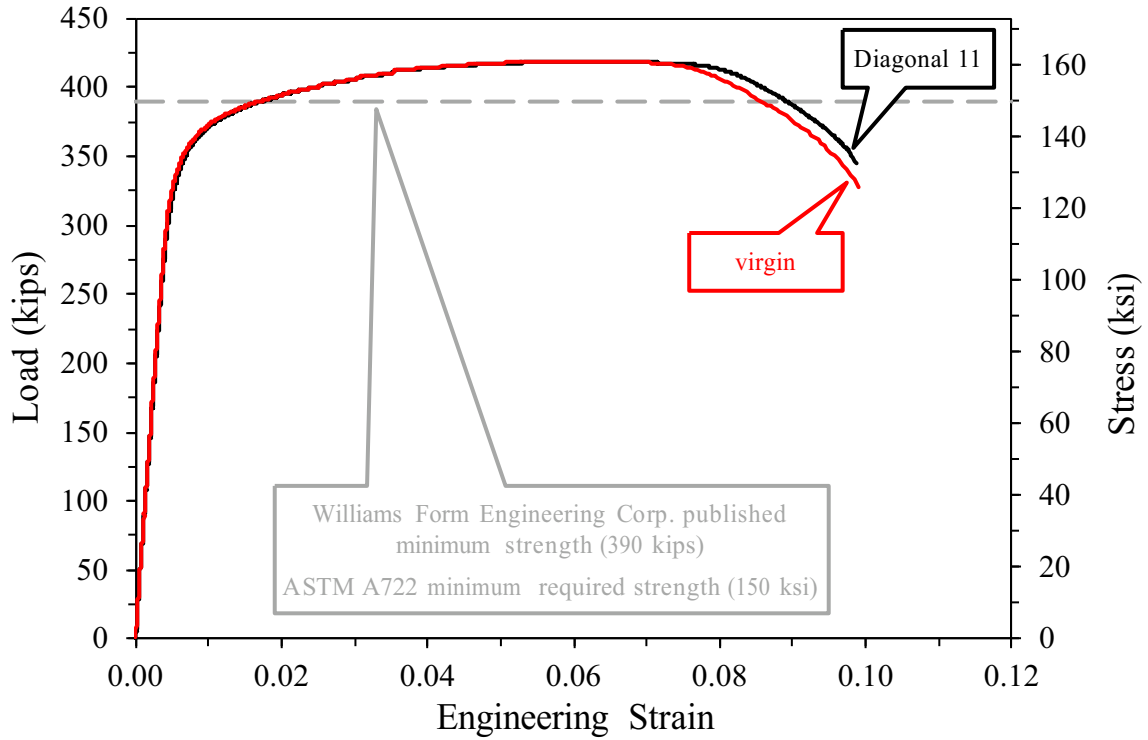


Figure 33. Load and stress versus strain for the full-size bars

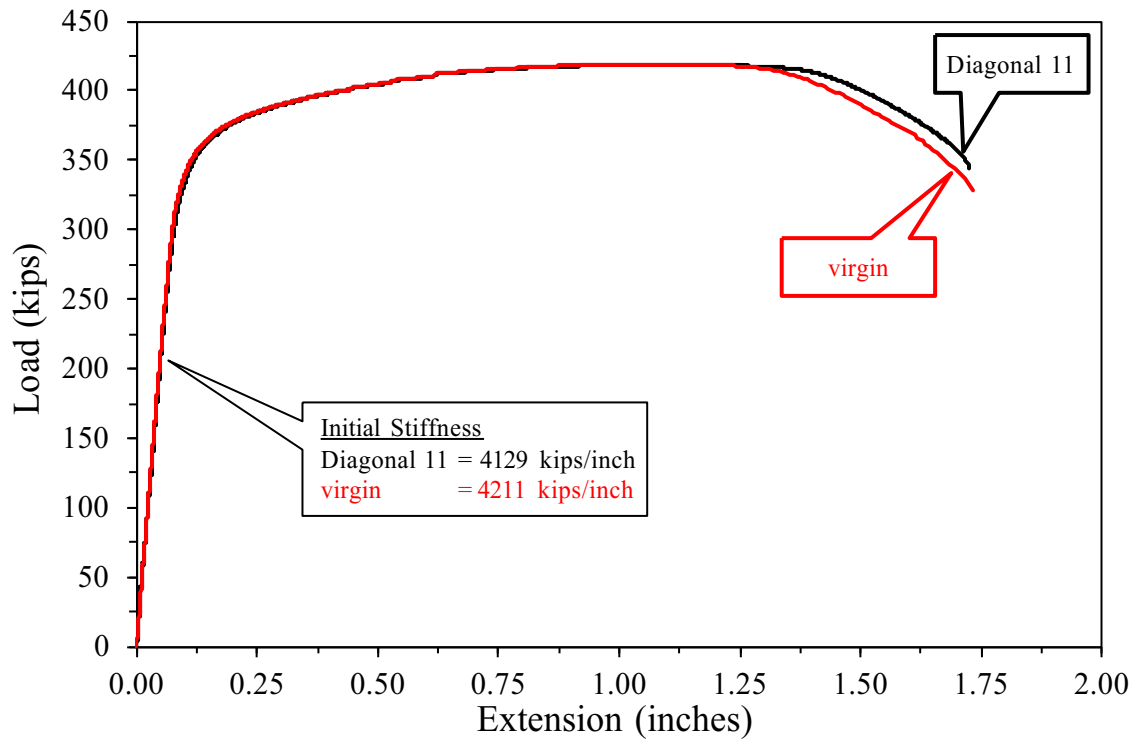


Figure 34. Load versus extension of the full-size bars



Figure 35. Photo of fractured Diagonal 11 bar



Figure 36. Photo of fractured virgin bar

Hardness Results

Hardness measurements were conducted following all guidelines of ASTM E18. The raw data collected from each rod cross-section are shown in Table 13 and Table 14 respectively for the virgin rod and the Diagonal 11 rod. The “reading” number correlates to the numbered position shown in Figure 26, and the pass/fail criterion comes from ASTM E18 whereby indents cannot be located within 3 indent diameters from another indent, or 2.5 diameters from an edge. The spacing requirement was verified with an invert microscope, and there were some locations that failed the edge spacing requirement. A plot of the hardness variation is shown in Figure 37 where the data point represents the average of all valid readings at the same radial location and the plus/minus error bar represents one standard deviation for the same data. Data that failed the ASTM E18 spacing requirement was censored from any statistical calculations. The variation was similar between the two rods.

Table 13. Virgin rod hardness measurements.

Reading	Rockwell C Hardness	Pass or fail spacing requirement?	Reading	Rockwell C Hardness	Pass or fail spacing requirement?	Reading	Rockwell C Hardness	Pass or fail spacing requirement?
1	35.2	Fail	23	36.7	Pass	45	35.5	Pass
2	34.0	Fail	24	36.0	Pass	46	36.7	Pass
3	35.0	Pass	25	35.1	Pass	47	34.9	Pass
4	^a	—	26	36.8	Pass	48	34.4	Pass
5	36.2	Pass	27	36.5	Pass	49	33.6	Pass
6	36.4	Fail	28	36.8	Pass	50	34.6	Pass
7	37.4	Fail	29	36.7	Pass	51	34.8	Pass
8	35.1	Fail	30	37.6	Pass	52	34.6	Pass
9	36.9	Pass	31	36.2	Pass	53	35.1	Pass
10	36.5	Pass	32	35.8	Pass	54	34.7	Pass
11	36.2	Pass	33	35.5	Pass	55	34.7	Pass
12	36.5	Pass	34	36.8	Pass	56	33.3	Pass
13	35.6	Pass	35	36.3	Pass	57	33.8	Pass
14	36.1	Pass	36	37.3	Pass	58	34.4	Pass
15	36.7	Pass	37	36.3	Pass	59	34.4	Pass
16	37.1	Pass	38	36.7	Pass	60	33.8	Pass
17	38.0	Pass	39	35.8	Pass	61	35.2	Pass
18	37.6	Pass	40	35.4	Pass	62	34.2	Pass
19	37.3	Pass	41	34.5	Pass	63	34.8	Pass
20	37.5	Pass	42	36.7	Pass	64	34.0	Pass
21	36.5	Pass	43	36.4	Pass	65	35.1	Pass
22	36.7	Pass	44	36.0	Pass	—	—	—

^aToo close to edge to measure.

— No data to report.

Table 14. Diagonal 11 rod hardness measurements.

Reading	Rockwell C Hardness	Pass or fail spacing requirement?	Reading	Rockwell C Hardness	Pass or fail spacing requirement?	Reading	Rockwell C Hardness	Pass or fail spacing requirement?
1	34.6	Fail	23	37.4	Pass	45	35.6	Pass
2	35.2	Fail	24	37.0	Pass	46	35.3	Pass
3	34.9	Pass	25	37.1	Pass	47	35.6	Pass
4	^a	—	26	37.1	Pass	48	36.0	Pass
5	34.1	Pass	27	37.1	Pass	49	34.4	Pass
6	35.5	Pass	28	36.0	Pass	50	34.5	Pass
7	36.4	Fail	29	35.6	Pass	51	34.1	Pass
8	^a	—	30	37.3	Pass	52	34.2	Pass
9	36.8	Pass	31	35.8	Pass	53	35.2	Pass
10	36.8	Pass	32	37.2	Pass	54	34.3	Pass
11	36.5	Pass	33	38.0	Pass	55	34.8	Pass
12	36.5	Pass	34	36.1	Pass	56	34.9	Pass
13	35.9	Pass	35	36.1	Pass	57	35.6	Pass
14	36.6	Pass	36	35.6	Pass	58	34.5	Pass
15	35.3	Pass	37	35.9	Pass	59	34.0	Pass
16	36.2	Pass	38	35.5	Pass	60	34.2	Pass
17	36.9	Pass	39	36.8	Pass	61	33.1	Pass
18	37.3	Pass	40	37.1	Pass	62	34.5	Pass
19	37.6	Pass	41	35.8	Pass	63	33.5	Pass
20	36.6	Pass	42	37.4	Pass	64	34.5	Pass
21	37.2	Pass	43	34.9	Pass	65	33.5	Pass
22	37.8	Pass	44	34.5	Pass	—	—	—

^aToo close to edge to measure.

—No data to report.

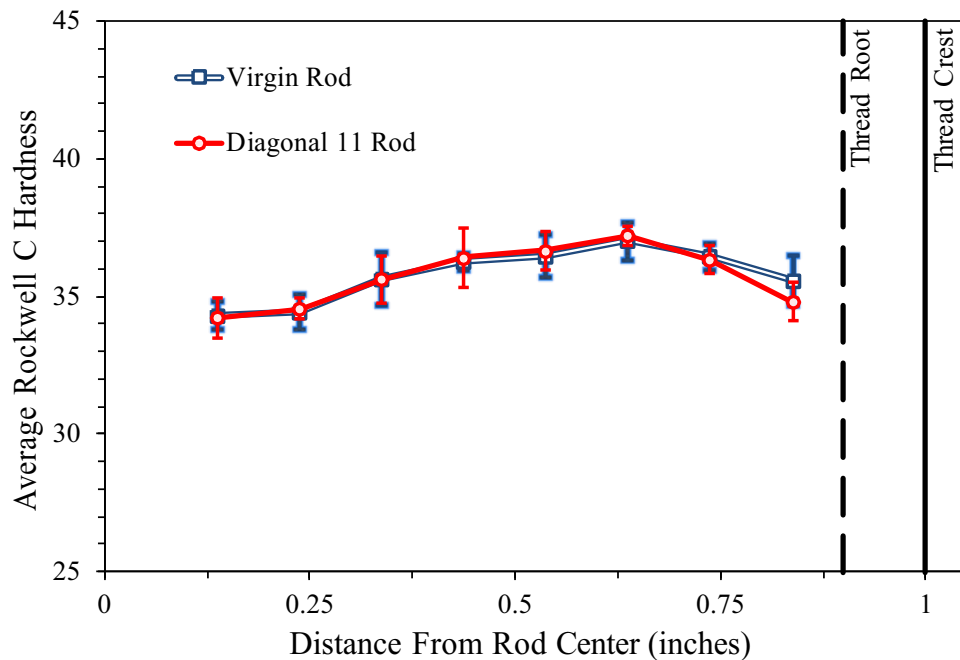


Figure 37. Graph of radial distribution of Rockwell C hardness for both rods

Chemical Assessment Results

ASTM A722 has chemical requirements controlling the limits of phosphorus and sulfur in the steel. To check composition of these two elements, the backside of the hardness specimens was used for sampling. Chemical assessment was performed in a glow discharge spectrometerⁿ following all requirements of ASTM E415^o and E1019^p. The results are shown in Table 15.

Table 15. PT rod chemical composition

Specimen	Phosphorus	Sulfur
Virgin	0.012	0.018
Diagonal 11	0.012	0.018
ASTM A722	≤ 0.040	≤ 0.050

ⁿ A glow discharge spectrometer is an instrument that excites atoms on the surface of a material and, through assessment of the resulting wavelengths and intensity of light emitted, reports the type and quantity of elements present in the material.

^o ASTM E415. (2017). “Standard Test Method for Analysis of Carbon and Low-Alloy Steel by Spark Atomic Emission Spectrometry.” ASTM Annual Book of Standards 03.05. ASTM International. West Conshohocken, PA.

^p ASTM E415. (2017). “Standard Test Methods for Determination of Carbon, Sulfur, Nitrogen, and Oxygen in Steel, Iron, Nickel, and Cobalt Alloys by Various Combustion and Inert Gas Fusion Techniques.” ASTM Annual Book of Standards 03.05. ASTM International. West Conshohocken, PA.

REINFORCING BARS

This section describes the reinforcing bar evidence that was received and the associated testing that was completed. Four sets of reinforcing bars were received. Each set of bars contained three bar samples of a given size. The bar sizes were #5, #7, #8, and #11. The reinforcing bars should meet ASTM A615^q requirements.

Documentation

Photographs of the #5, #7, #8, and #11 bar sets are shown in Figure 38, Figure 39, Figure 40, and Figure 41, respectively. Each sample was given a unique identifier, which are shown in the figures below. The #5 and #8 bars were recovered from the deck/diaphragm region below diagonal 11. The #11 bars were extracted from the upper portion of vertical 12, close to where the member connected to the canopy. The exact location from which the #7 bars were extracted is unknown.

Each bar sample was inspected to determine its suitability for tensile testing. Specifically, bars were inspected to determine their geometric linearity or straightness. It was determined that no portions of the #7 bar samples or sample #8-2 were suitable for testing due to the out-of-straightness of these bars. The remaining bar samples were all determined to have regions sufficiently straight to be suitable for uniaxial tension testing.



Figure 38. #5 bars received

^q ASTM A615. (2018). “*Standard Specification for Deformed and Plain Carbon-Steel Bars for Concrete Reinforcement.*” ASTM Annual Book of Standards 01.04. ASTM International. West Conshohocken, PA.



Figure 39. #7 bars received



Figure 40. #8 bars received



Figure 41. #11 bars received

Tension Test Method Description

The reinforcing bar testing was performed in accordance to ASTM A370 using the 220-kip testing frame shown in Figure 29 and the same loading program previously described for the PT rod testing. In terms of reinforcing bars, ASTM A615 requires elongation measured over an 8-inch gauge length and requires 2 additional bar diameters of bar length between the end of the gauge length and grips. All the bars tested meet this minimum length requirement, however, the grip-to-grip distance for each specimen varied slightly. The grip-to-grip distance defined the reduced section length, which was used by the loading program to calculate the loading rate. Strain was measured with a video extensometer over an 8.000-inch gauge length, centered on the grip-to-grip distance.

Tension Test Results

Figures 42, 43, and 44 show the stress versus strain results, respectively, for the #5, #8, and #11 bars. The pertinent data for each of the specimens is reported in Table 16. Yield strength was determined by the 0.2% offset method defined in ASTM A370, tensile strength was based on the maximum stress achieved, and elongation at fracture was the final strain measured before significant load drop from fracture.

Specimens #11-2 and #11-3 fractured near the grips and thus outside the 8-inch gauge length. For these two specimens, the reported elongation is not fully representative of the material since it does not capture the necking of the specimen prior to fracture. This also explains the final load drop for these two specimens in Figure 44 because load was dropping as necking occurred outside the gauge length, thus keeping the strain nearly constant within the gauge length. Additional post-processing of the video extensometer data could be possible with an increased gauge length; however, since the measured elongation within the 8.000-inch gauge length was greater than the ASTM A615 requirement, this additional processing was not completed.

Photographs of the failed #5, #8, and #11 specimens are shown in Figure 45, Figure 46, and Figure 47, respectively.

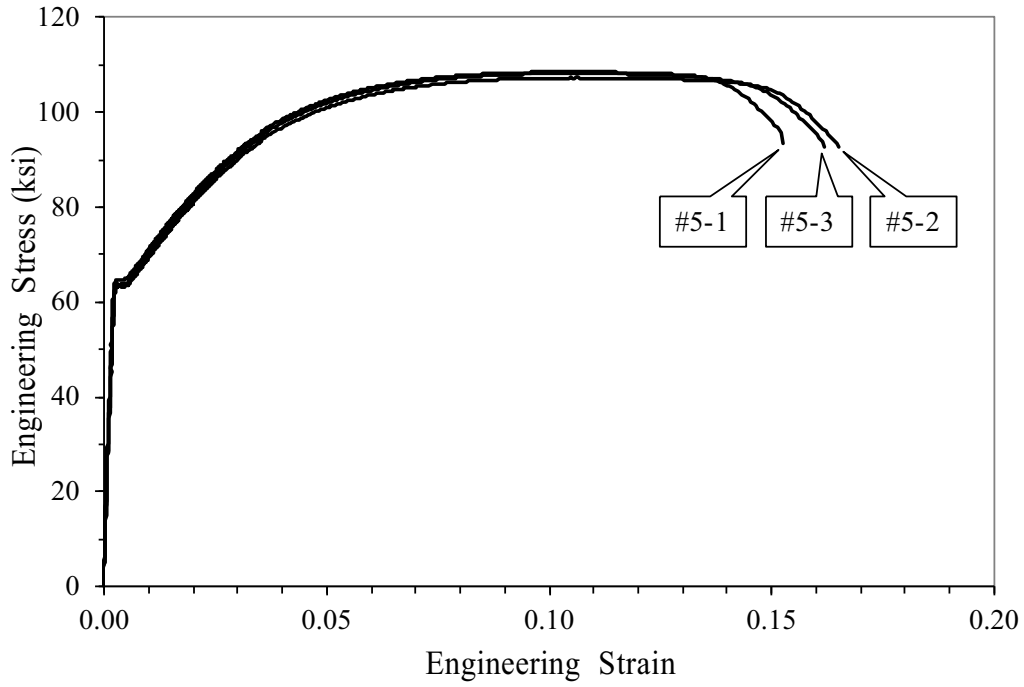


Figure 42. Stress versus strain results for #5 reinforcing bars

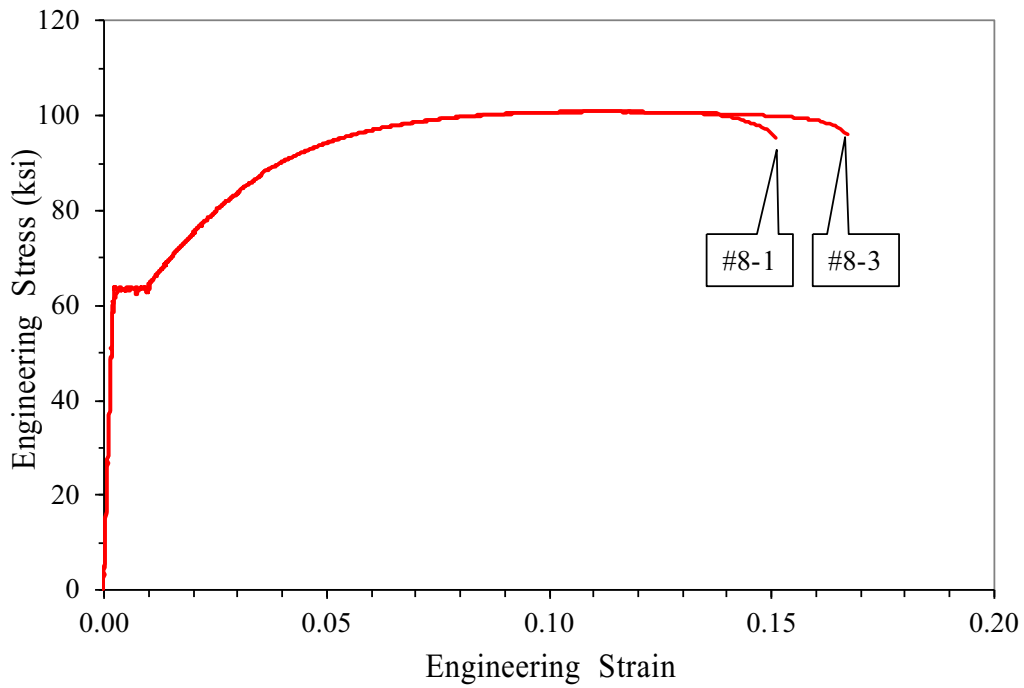


Figure 43. Stress versus strain results for #8 reinforcing bars

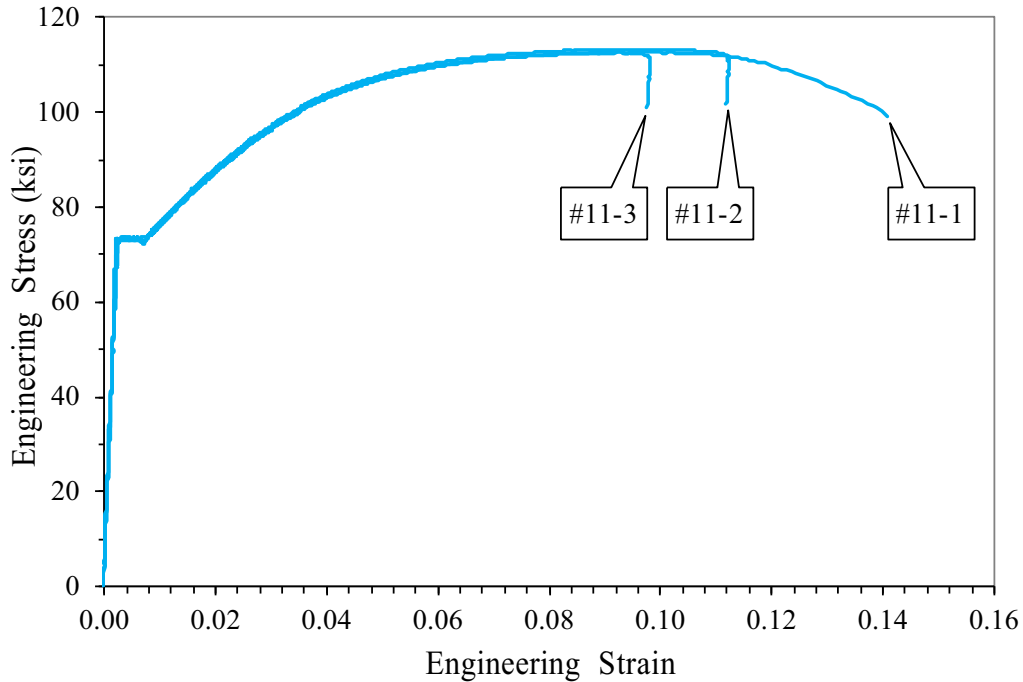


Figure 44. Stress versus strain results for #11 reinforcing bars

Table 16. Summary results of reinforcing bars

Specimen	Yield Strength (ksi)	Tensile Strength (ksi)	Elongation at Fracture (percent)
#5-1	64.7	108.5	15.25
#5-2	63.2	107.3	16.52
#5-3	63.7	108.2	16.19
#8-1	63.4	100.9	15.08
#8-3	63.4	100.8	16.71
#11-1	73.1	112.6	14.09
#11-2	73.6	113.2	11.23 ^b
#11-3	72.8	112.6	9.81 ^b
ASTM A615	≥ 60	≥ 90	^a

^aMinimum requirement is 9%, 8%, and 7%, respectively for #5, #8, and #11 bars.

^bFracture occurred outside the extensometer gauge length and punch marks, therefore reported elongation is not the true elongation, but represents a minimum value the material did achieve.



Figure 45. Photographs of fractured #5 bar specimens



Figure 46. Photographs of fractured #8 bar specimens



Figure 47. Photographs of fractured #11 bar specimens